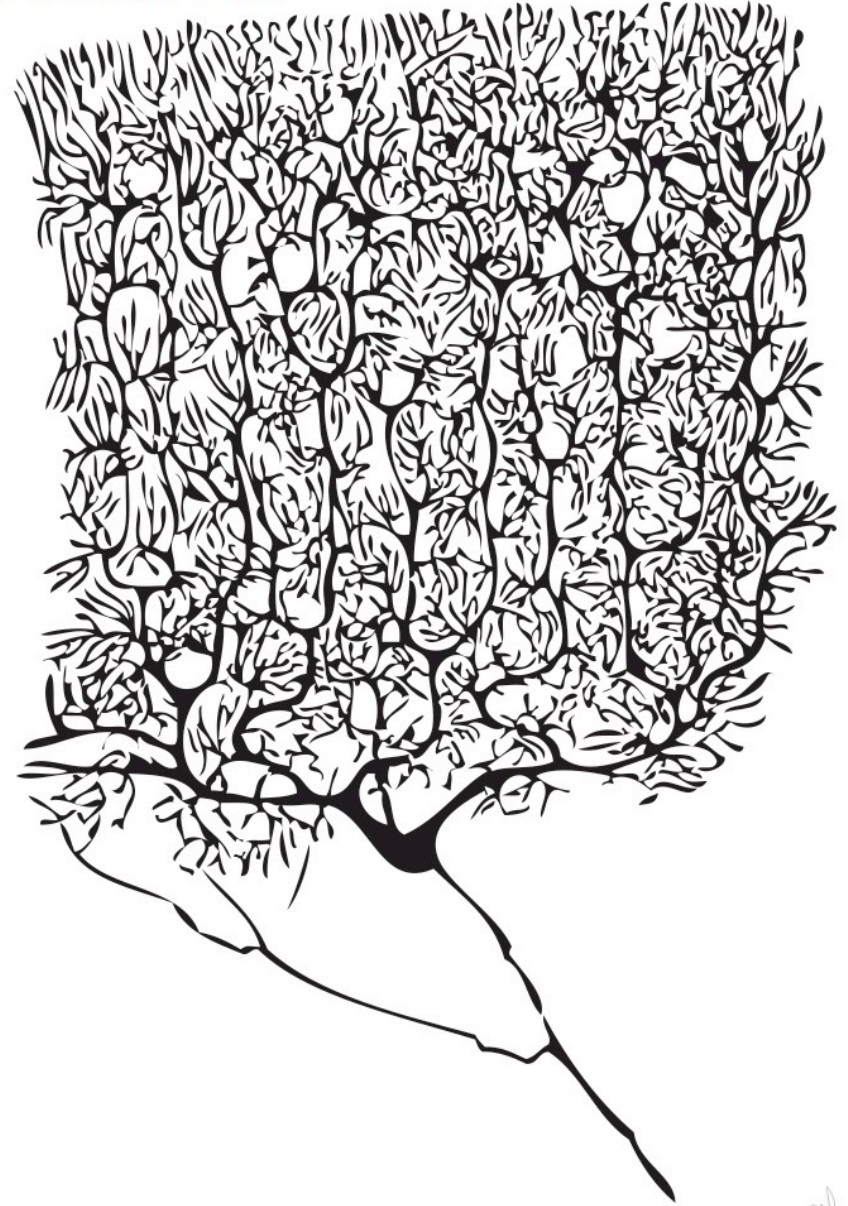


Cellular Electrodynamics

Santiago Ramón y Cajal (1852-1934)



Instructor:

Prof. Christopher Bergevin (cberge@yorku.ca)

Website:

<http://www.yorku.ca/cberge/4080W2020.html>

York University
Winter 2020

BPHS 4080 Lecture 20

Reference/Acknowledgement:

- TF Weiss (Cellular Biophysics)
- D Freeman

A small, stylized signature or logo located in the bottom right corner of the slide, consisting of a few overlapping loops and lines.

Summary: HH Equations

$$\frac{1}{2\pi a(r_o + r_i)} \frac{\partial^2 V_m}{\partial z^2} = C_m \frac{\partial V_m}{\partial t} + G_K(V_m, t) (V_m - V_K) + G_{Na}(V_m, t) (V_m - V_{Na}) + G_L(V_m - V_L)$$

$$G_K(V_m, t) = \bar{G}_K n^4(V_m, t)$$

$$G_{Na}(V_m, t) = \bar{G}_{Na} m^3(V_m, t) h(V_m, t)$$

$$n(V_m, t) + \tau_n(V_m) \frac{dn(V_m, t)}{dt} = n_\infty(V_m)$$

$$m(V_m, t) + \tau_m(V_m) \frac{dm(V_m, t)}{dt} = m_\infty(V_m)$$

$$h(V_m, t) + \tau_h(V_m) \frac{dh(V_m, t)}{dt} = h_\infty(V_m)$$

$$\tau_x \frac{dx}{dt} + x = x_\infty \quad \frac{dx}{dt} = \alpha_x(1-x) - \beta_x x$$

$$x_\infty = \alpha_x / (\alpha_x + \beta_x) \text{ and } \tau_x = 1 / (\alpha_x + \beta_x)$$

$$\alpha_m = \frac{-0.1(V_m + 35)}{e^{-0.1(V_m + 35)} - 1},$$

$$\beta_m = 4e^{-(V_m + 60)/18},$$

$$\alpha_h = 0.07e^{-0.05(V_m + 60)},$$

$$\beta_h = \frac{1}{1 + e^{-0.1(V_m + 30)}},$$

$$\alpha_n = \frac{-0.01(V_m + 50)}{e^{-0.1(V_m + 50)} - 1},$$

$$\beta_n = 0.125e^{-0.0125(V_m + 60)},$$

Question:

So what do m , h , and n physically represent?

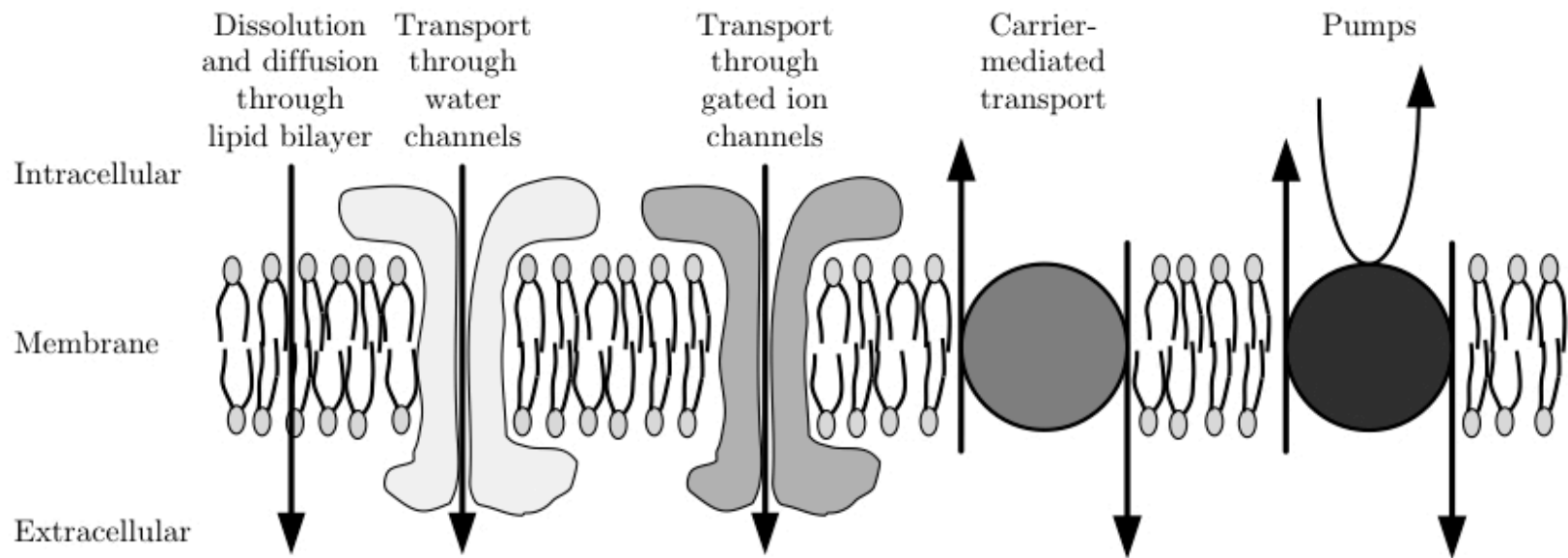


Figure 2.19

→ Notion of an ion channel



March 19, 2016 issue
(vol. 438, num. 8981)



“Susumu Tonegawa used a technique known as optogenetics, which activates clusters of neurons by shining light on them. As they report in *Nature*, the researchers prepared seven month-old Alzheimer’s mice by injecting a harmless virus into the rodents’ dentate gyrus, a part of the hippocampus that helps to store fearful memories. The virus contains a gene for channelrhodopsin-2, a light-sensitive protein which forms pores in the cell membranes of neurons infected with the virus. These pores are closed in the dark, but open in response to blue light, flooding neurons with positively charged ions. The resulting pulse of current makes the neurons fire. During their experiments, the researchers were able to illuminate the infected neurons of the mice using optical fibres implanted in their brains.”

misleading researchers. However, this has not proved a significant problem in the physical sciences. Manuscripts submitted to arXiv (and bioRxiv) are checked to ensure that they are not crank science. And, as Paul Ginsparg, who founded arXiv, noted in a talk at ASA/Pbio, researchers are more careful to check un-peer-reviewed papers before making them public. Furthermore, journal peer review is not infallible: poor science routinely slips through the net.

In any case, there is no reason to prevent a preprint from being reviewed after it is uploaded. One example of this is *Discrete Analysis*, a mathematics journal launched on March 1st by Tim Gowers of the University of Cambridge. This is an “overlay” journal, a sort of stripped-down online publication which provides links to papers in arXiv and sends submitted manuscripts out for peer review at no cost to the author (the administration cost of around \$10 per submission is covered by the journal).

Agency of change

Michael Eisen of the University of California, Berkeley, a zealous proponent of open science, argues that the traditional publication model is outmoded. Researchers are far more likely to use keyword searches in Google to find papers relevant to their work than to leaf through printed journals. Preprints, he says, put researchers back in the driving seat: “Instead of being told by journals what papers to review, we review papers useful to us.”

There are signs that researchers might be tiring of the grip that the elite journals have on the biomedical sciences. Over 12,000 people have so far signed the San Francisco Declaration on Research Assessment (DORA), which began in 2012 as a commitment for research to be assessed “on its own merits rather than on the basis of the journal in which the research is published”. If the science community takes this notion seriously, more researchers might be persuaded of the value of publishing preprints (because journal publications will be less important). A report to the British government on open access to research, published in February by the Department for Business, Innovation and Skills, recommends all universities in the country now sign DORA.

The wide adoption of preprints, however, depends ultimately on paymasters and interview panels moving away from judging the worth of a scientist by the number of publications in elite journals that appear on his cv. While few funding agencies consider preprints to be formally published work, some have at least made tentative moves towards assessing a scientist’s research more broadly. Medical research groups in America, Britain and Australia, for example, have emphasised that scientific work will be judged by its quality,

not by the reputation of the journal it is published in. That will certainly be more onerous for committees than counting up the “right” sort of papers. But if more researchers feel comfortable about uploading their work to preprint servers, it will break the stranglehold of elite journals on biomedical science and accelerate discovery. That would save millions of dollars. More importantly, it would save lives. ■

Restoring lost memories

Total recall

Missing memories have been restored in mice with Alzheimer’s disease

SOME mice can easily remember where they hide food, but not those genetically engineered to develop Alzheimer’s disease. Like humans they become forgetful. By the time these mice are seven months old they are unable to remember, for example, which arm of a maze they have explored before. Two months later, their brains are riddled with amyloid beta, the protein “plaques” that also characterise the latter stage of the disease in humans.

Now researchers have managed to restore memories to mice with Alzheimer’s. This helps provide more evidence about how memories are lost during the early stages of the disease and may point to how, some time in the future, those memories might be brought back.

Susumu Tonegawa and his colleagues at the Massachusetts Institute of Technology used a technique known as optogenetics, which activates clusters of neurons by shining light on them. As they report in *Nature*, the researchers prepared seven-month-old Alzheimer’s mice by injecting a harmless virus into the rodents’ dentate gyrus, a part of the hippocampus that helps to store fearful memories. The virus contains a gene for channelrhodopsin-2, a light-sensitive protein which forms pores in the cell membranes of neurons infected with the virus. These pores are closed in the dark, but open in response to blue light, flooding neurons with positively charged ions. The resulting pulse of current makes the neurons fire. During their experiments, the researchers were able to illuminate the infected neurons of the mice using optical fibres implanted in their brains.

Using a standard lab test of memory, a mouse was placed in a box and given a small electrical shock to its feet. Normal mice remember this and freeze in fear if put back in the box the following day, but mice with Alzheimer’s scamper about unfazed. Yet when the researchers stimulated the dentate gyrus of these mice with blue light,

they also froze, suggesting that they were now able to recall the original shock.

Holding on to a fearful memory in the long term, however, requires the brain to strengthen the nerve connections (synapses) that link memory of the box to experience of the shock. This process, known as long-term potentiation, goes awry in the brains of Alzheimer’s patients. Consistent with this idea, the Alzheimer’s mice did not freeze when placed in the box but only when their neurons were illuminated.

To help the Alzheimer’s mice consolidate and keep their memory of the electric shock, the team flashed their dentate gyrus with blue light at 100 hertz, a frequency known to induce long-term potentiation. After this the Alzheimer’s mice froze in the box for at least six consecutive days, suggesting they were able to remember the shock themselves.

Work by other groups has suggested that in its early stages, Alzheimer’s principally damages the brain’s ability to process and store memories. This new work, however, indicates that it is the brain’s ability to retrieve memories that is impaired. The distinction is far from an academic one. If memories are garbled before they are stored, they are lost for ever. But if Dr Tonegawa is right, then memories are correctly preserved in the brains of Alzheimer’s patients. That means it may be possible to rescue them—perhaps by adapting optogenetics for use in human sufferers. That remains a distant possibility for now.

But there is a more immediate consequence of the work for the estimated 40m people with the disease. Electrical stimulation of large areas of the brain of Alzheimer’s patients is already being tried, using electrodes implanted in the skull. But Dr Tonegawa’s team found that stimulating neurons in the dentate gyrus other than those directly involved with holding the fear memory prevented Alzheimer’s mice from remembering their shocks in the long term. That suggests that unless the technique can be refined, deep-brain stimulation may not be effective. ■



Remembering in a new light

“The virus contains a gene for channelrhodopsin-2, a light-sensitive protein which forms pores in the cell membranes of neurons infected with the virus. These pores are closed in the dark, but open in response to blue light, flooding neurons with positively charged ions. The resulting pulse of current makes the neurons fire.”

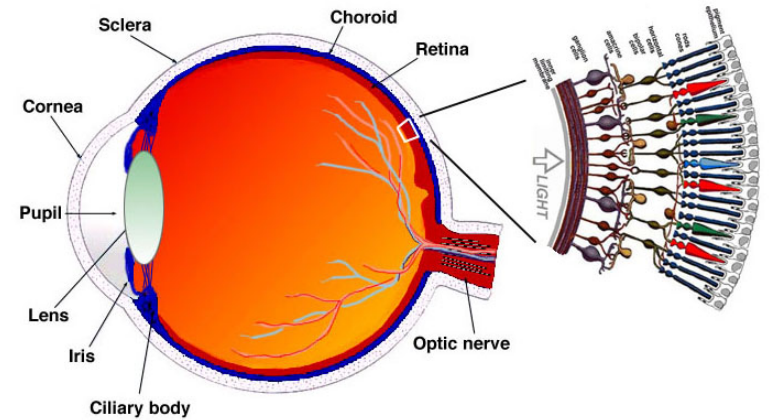


Fig. 1.1. A drawing of a section through the human eye with a schematic enlargement of the retina.

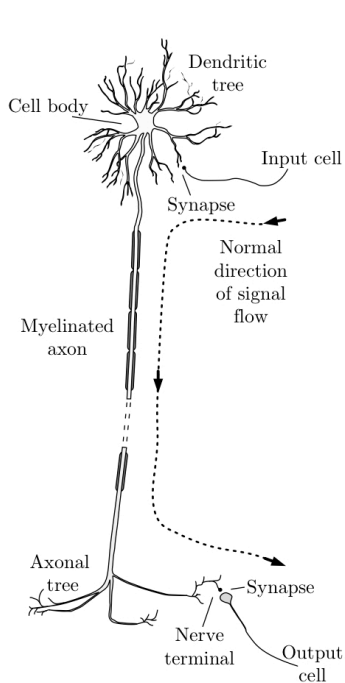


Figure 1.22

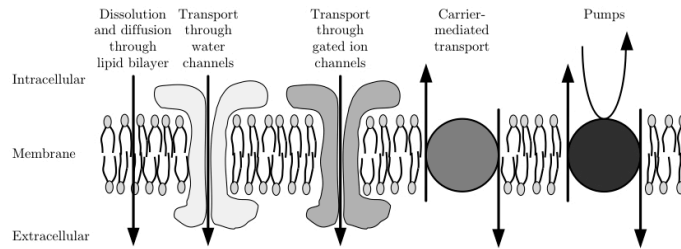
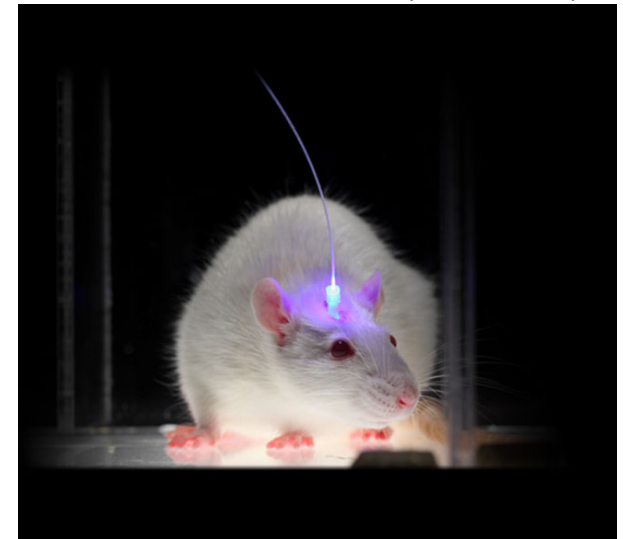


Figure 2.19



(see Lec.16ff)



<http://web.stanford.edu/group/dlab/optogenetics/>

Macroscopic Ionic Currents: HH Methodology

Voltage clamp

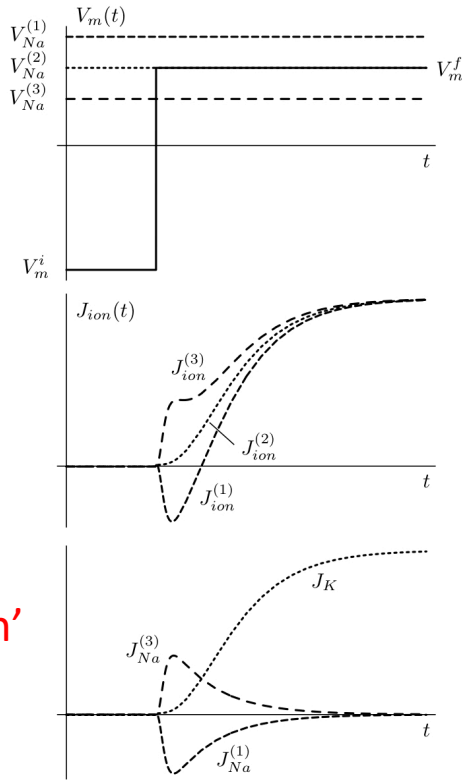


Figure 4.17

'subtraction'

NOTE: Other methods besides subtraction (e.g., TTX to block Na⁺ current, replace K⁺ w/ Cs⁺, etc...)

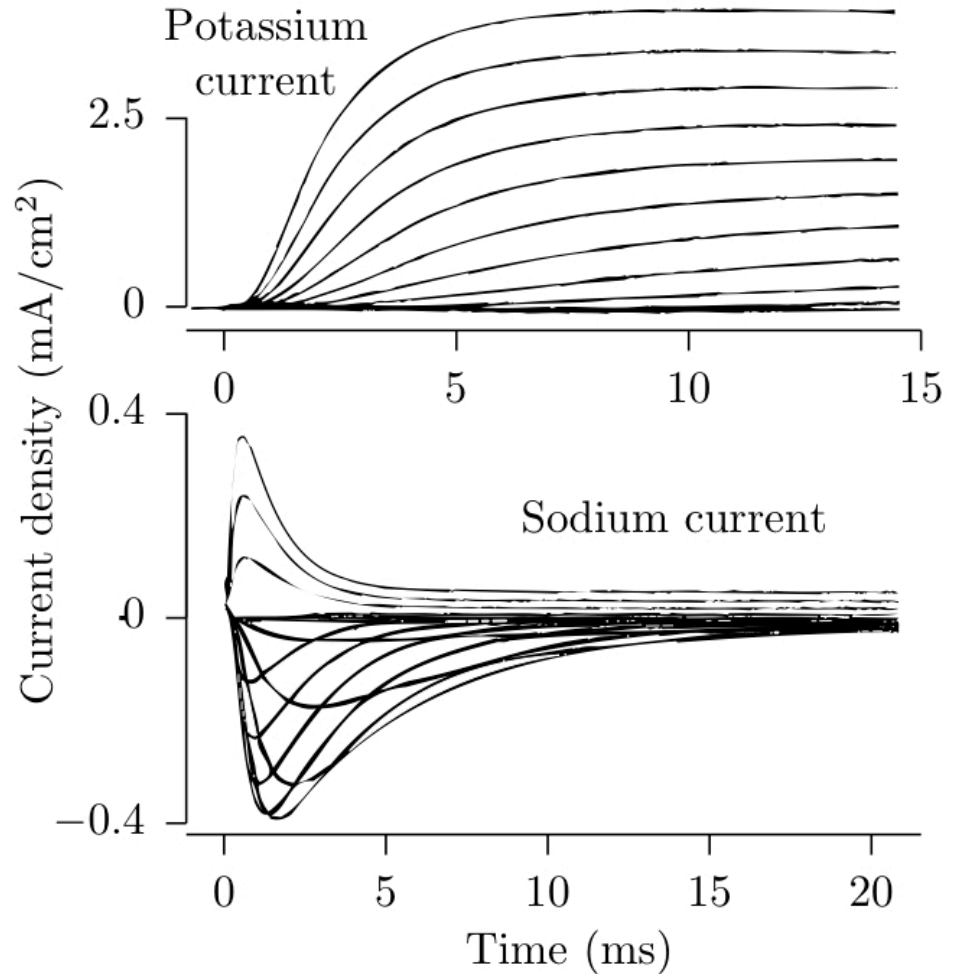


Figure 4.20

Macroscopic Ionic Currents: Selectivity

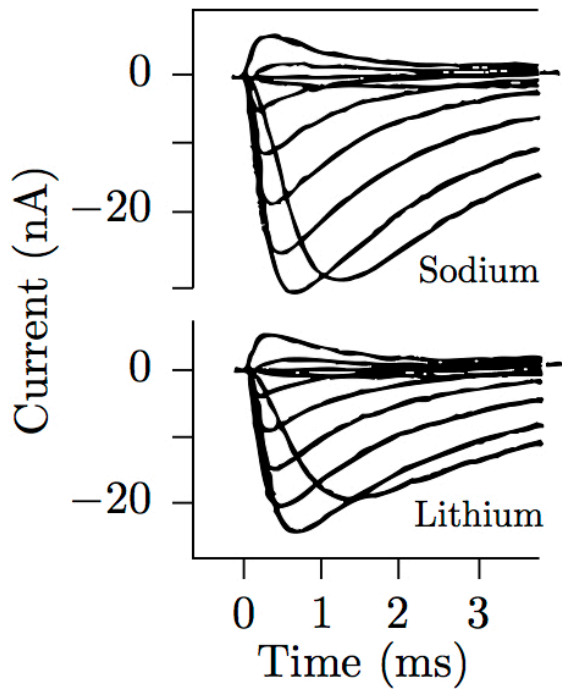


Figure 6.8

→ Ion channels 'prefer' certain ions, but are not necessarily exclusive

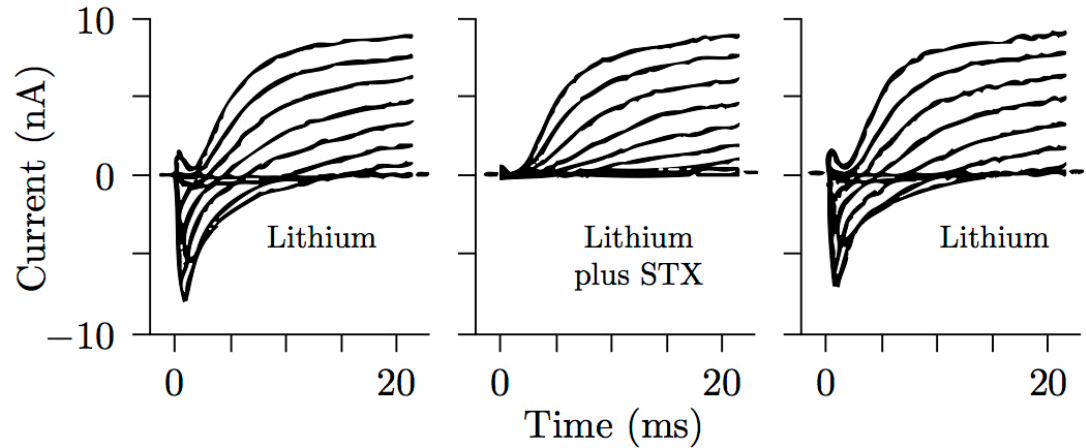


Figure 6.9

Table 6.1 (mod)

Na ⁺ channel Frog node		K ⁺ channel Frog node	
Ion <i>n</i>	P_n/P_{Na^+}	Ion <i>n</i>	P_n/P_{K^+}
Na ⁺	1.0	Tl ⁺	2.3
Li ⁺	0.93	K ⁺	1.0
Tl ⁺	0.33	Rb ⁺	0.91
NH ₄ ⁺	0.16	NH ₄ ⁺	0.13
K ⁺	0.086	Cs ⁺	< 0.077
Rb ⁺	< 0.012	Li ⁺	< 0.018
Cs ⁺	< 0.013	Na ⁺	< 0.10

Microscopic Current Mechanism

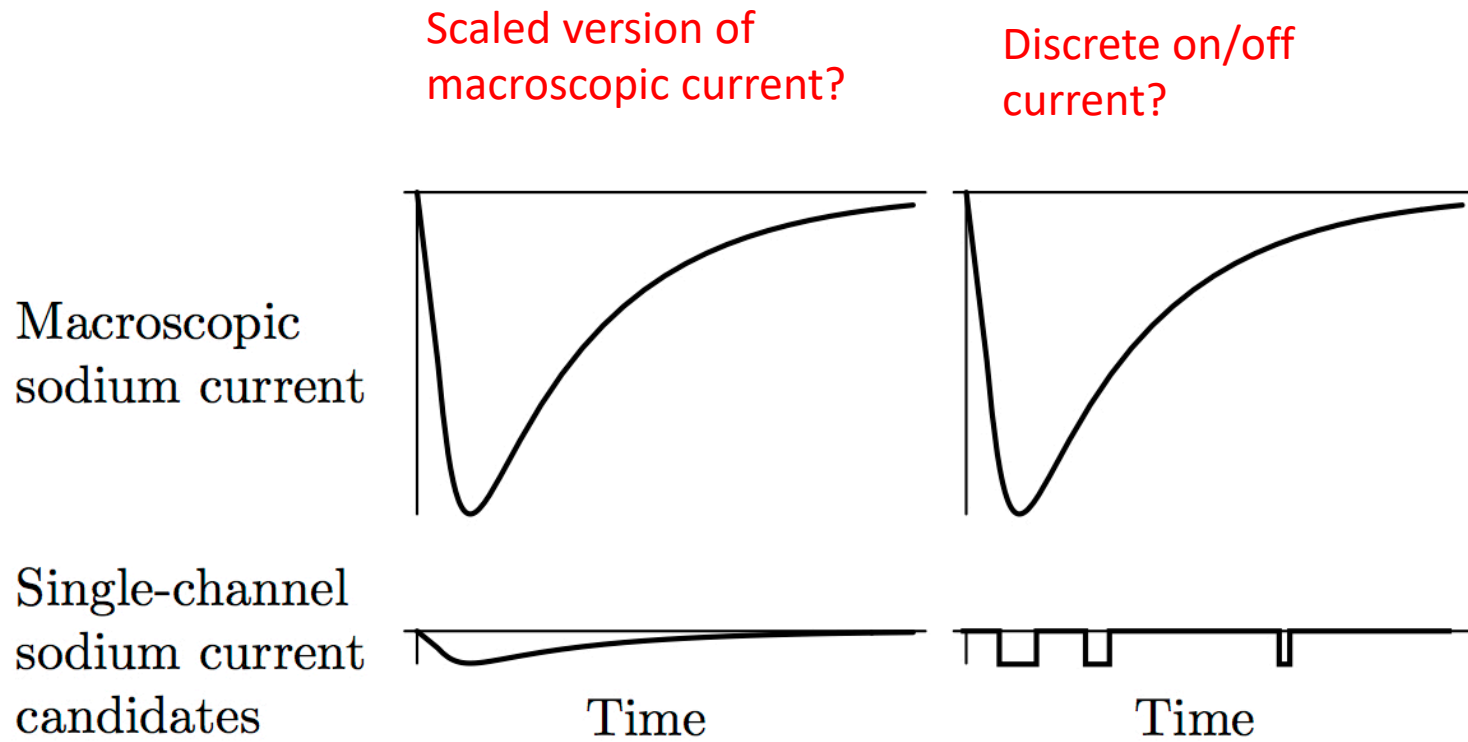
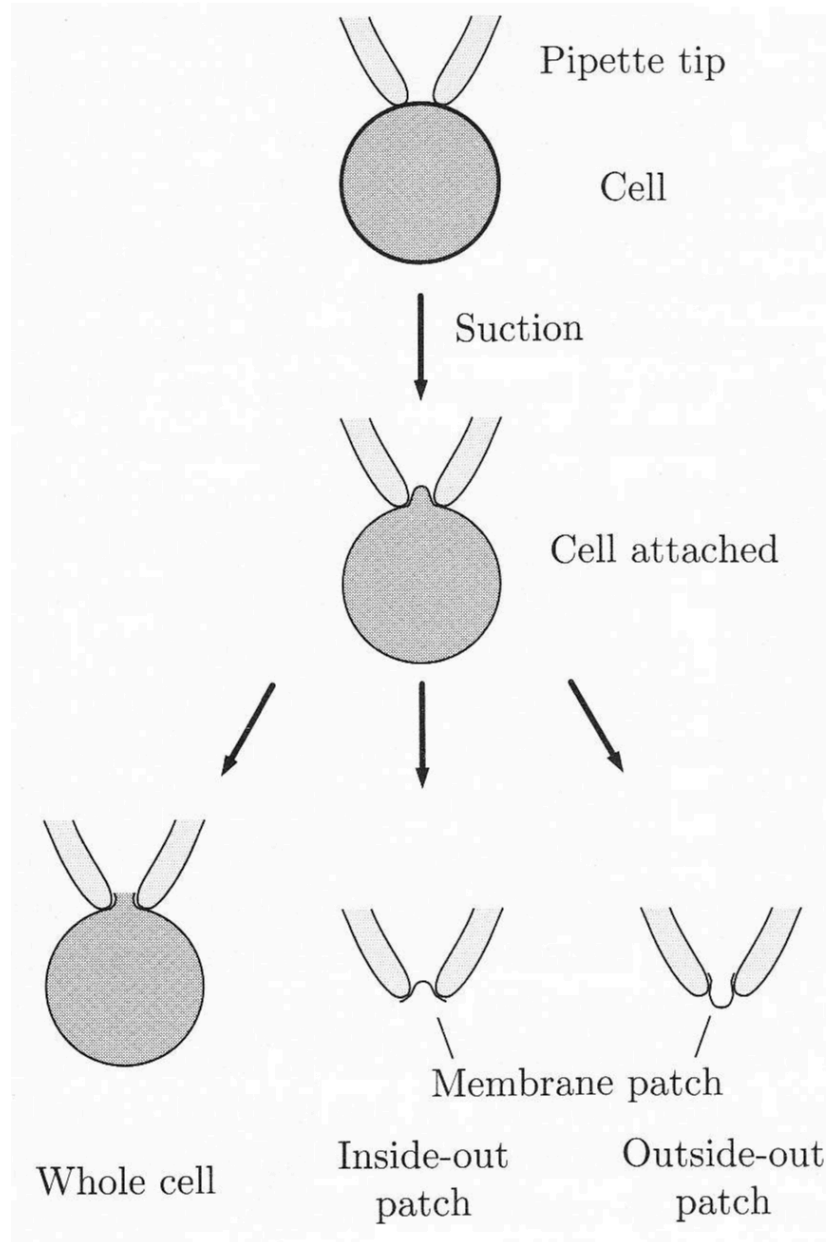


Figure 6.27

Patch Clamp



→ Refinement of voltage-clamp

Figure 6.1

Patch Clamp

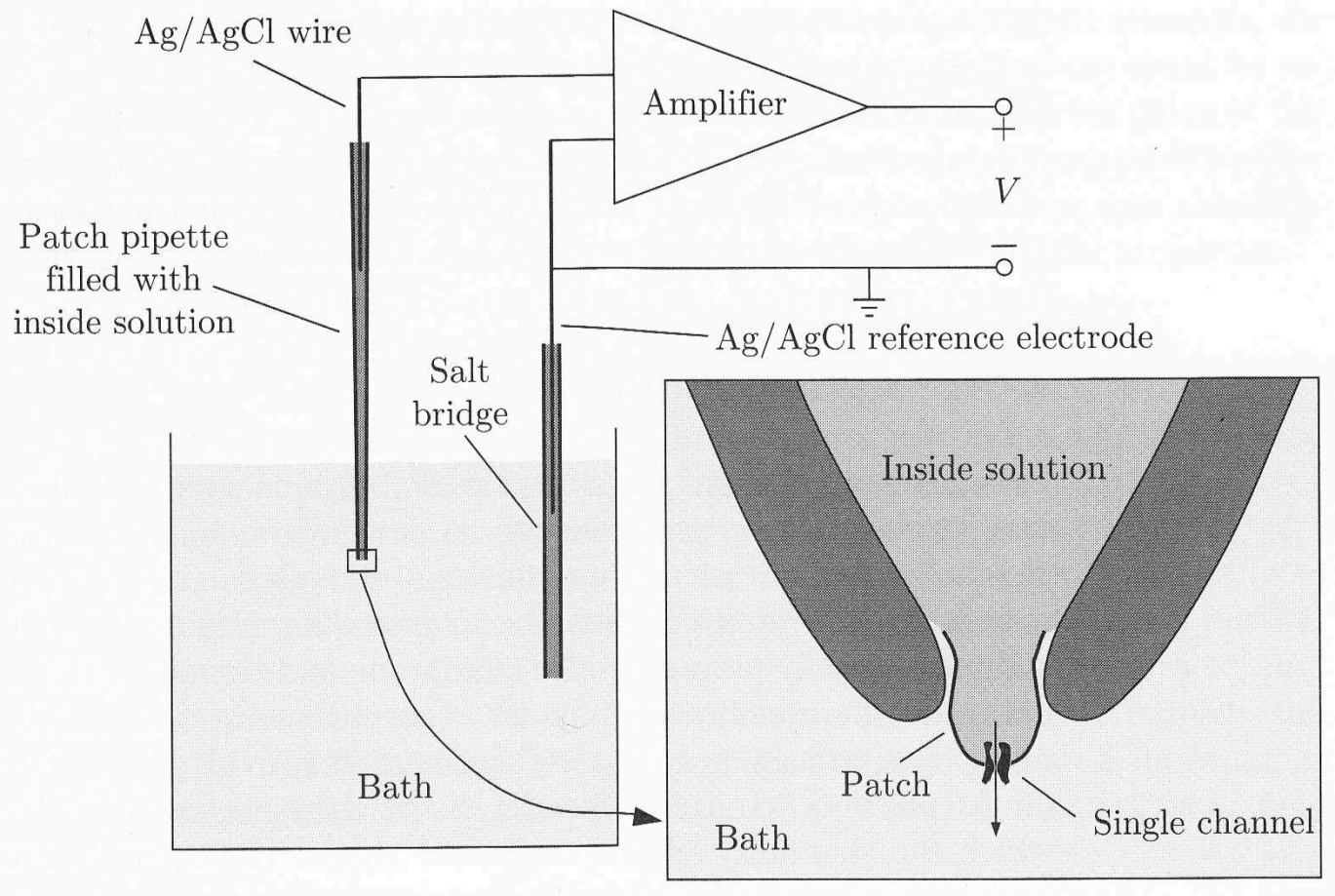
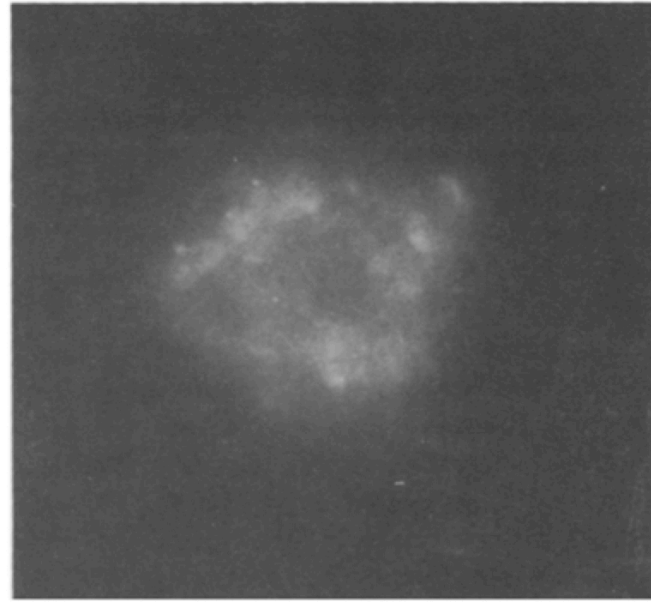
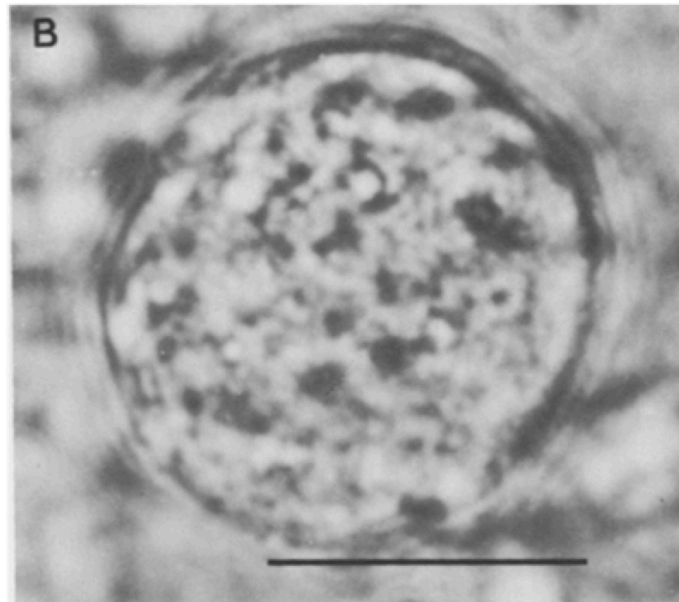
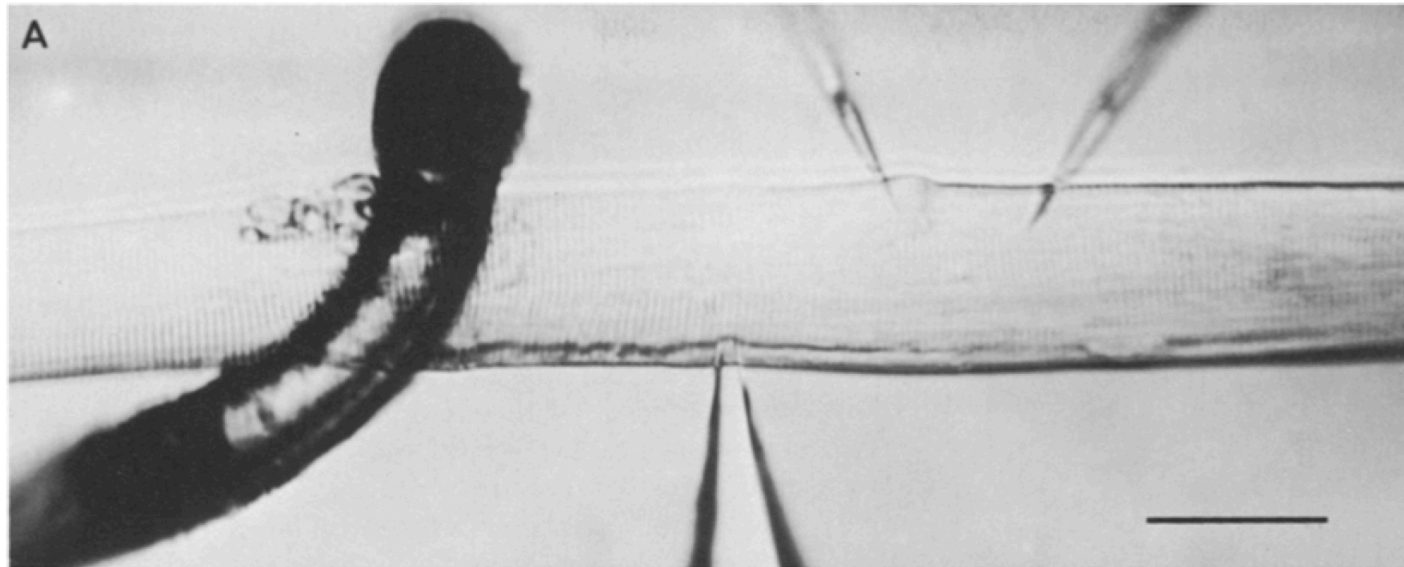


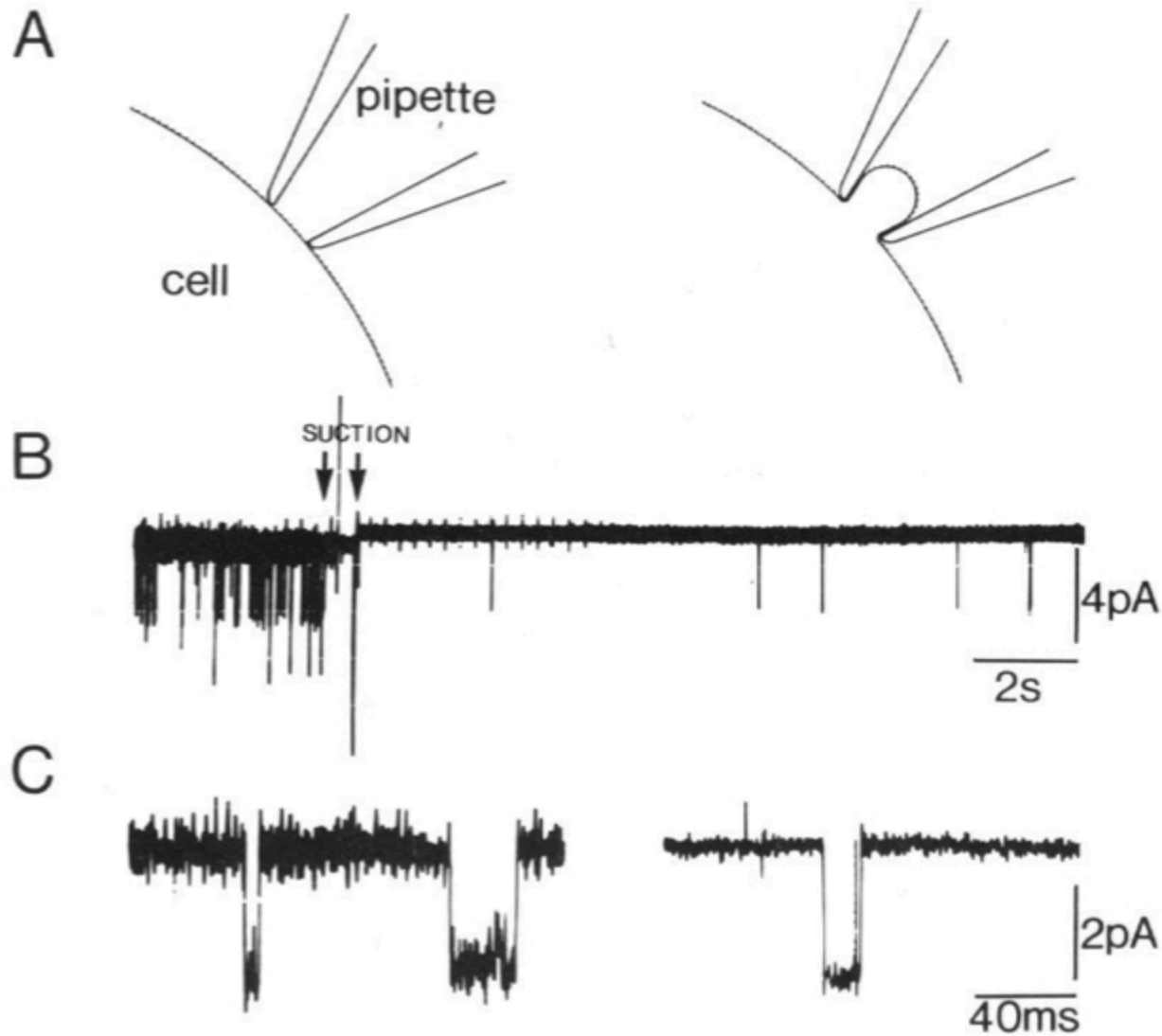
Figure 6.2

→ Goal is to isolate a single ion channel

Patch Clamp



Patch Clamp



→ Current through a single channel!

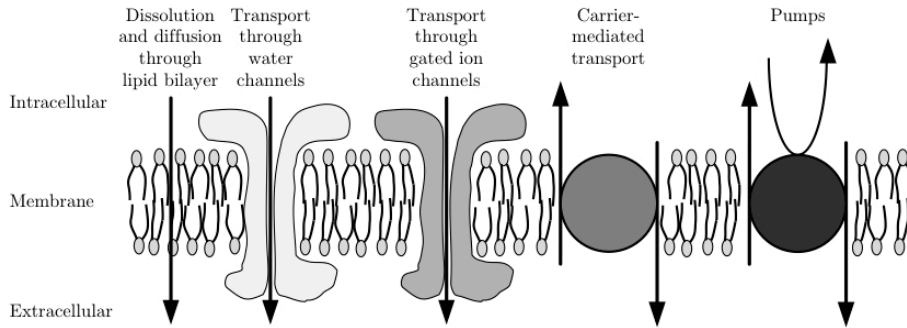
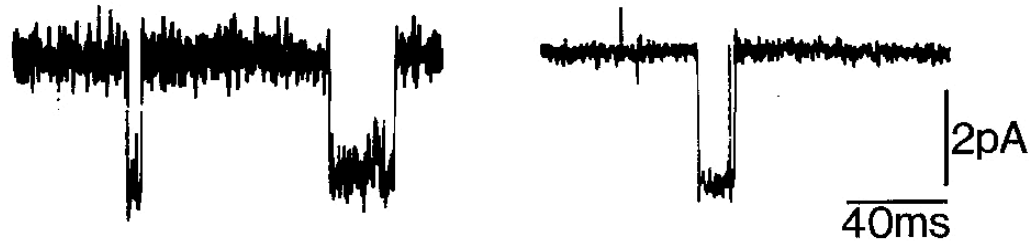
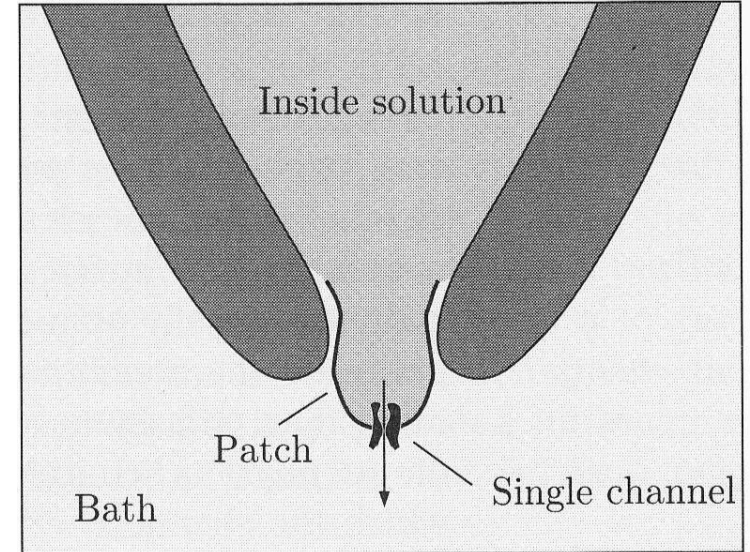
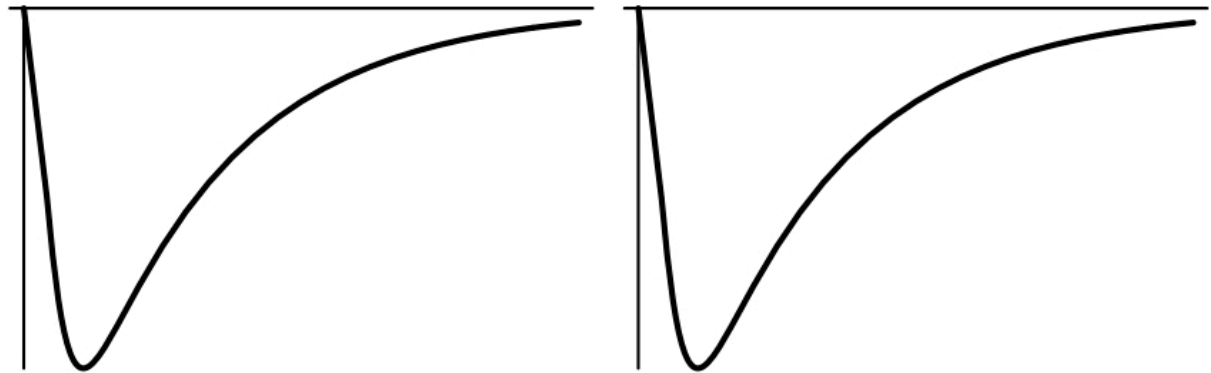


Figure 2.19



→ Single ion channel current appears 'gated' (i.e., on/off)

Macroscopic
sodium current



Single-channel
sodium current
candidates



Figure 6.27

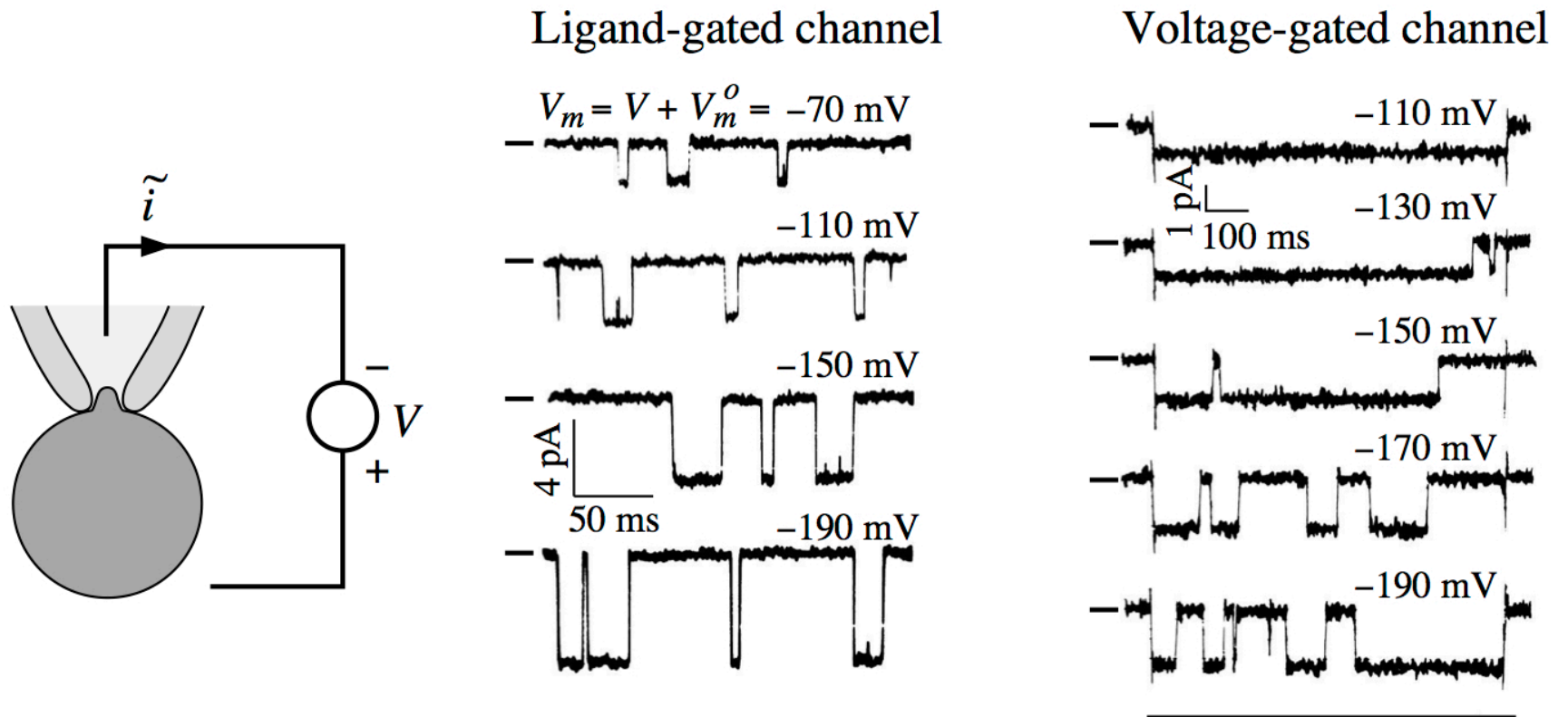
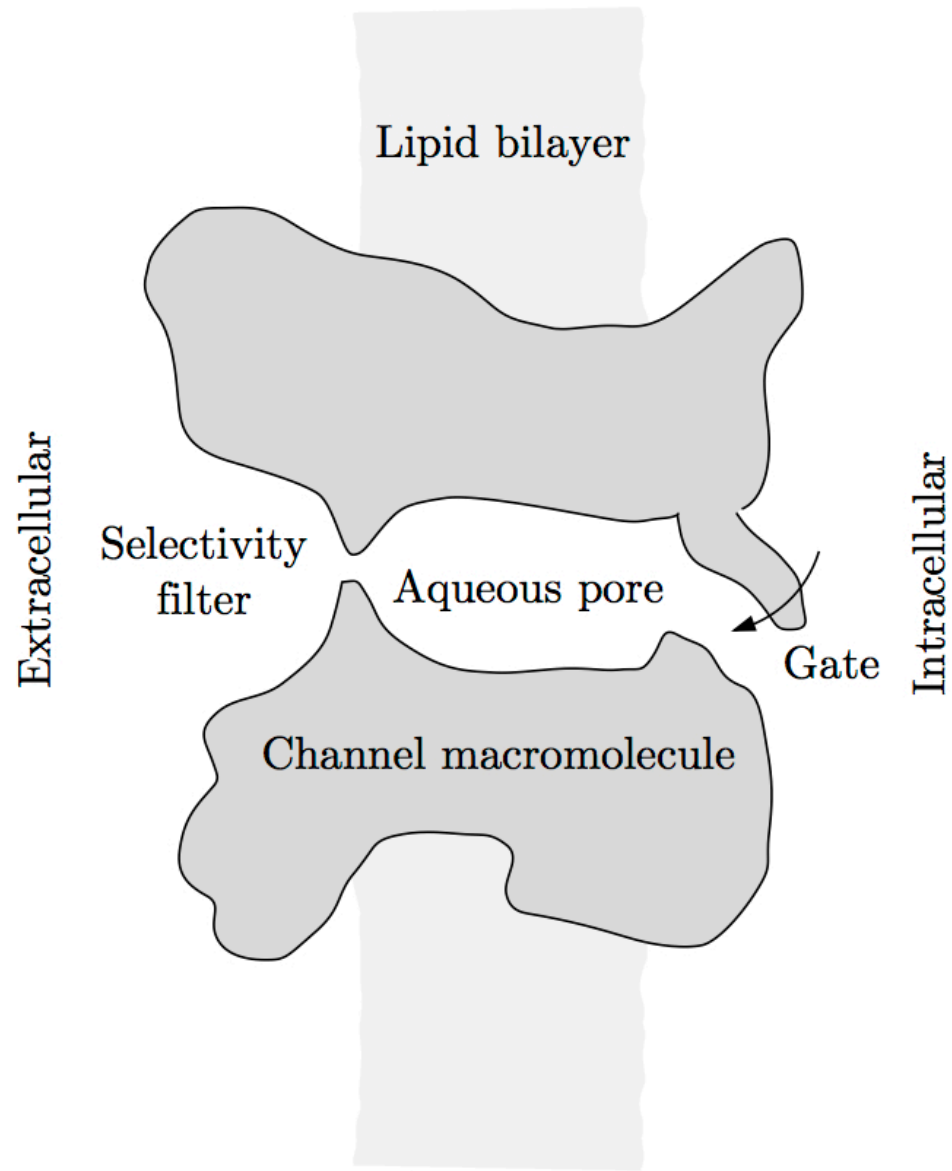


Figure 6.28

- Random nature of channels
- Voltage-gated channels more likely to be open when magnitude of potential increased
- Note change in current (both cases) with respect to holding potential

(Primitive) Ion Channel Model



Current types:

1. Ionic
2. Gating/capacitive

Figure 6.3

Current types

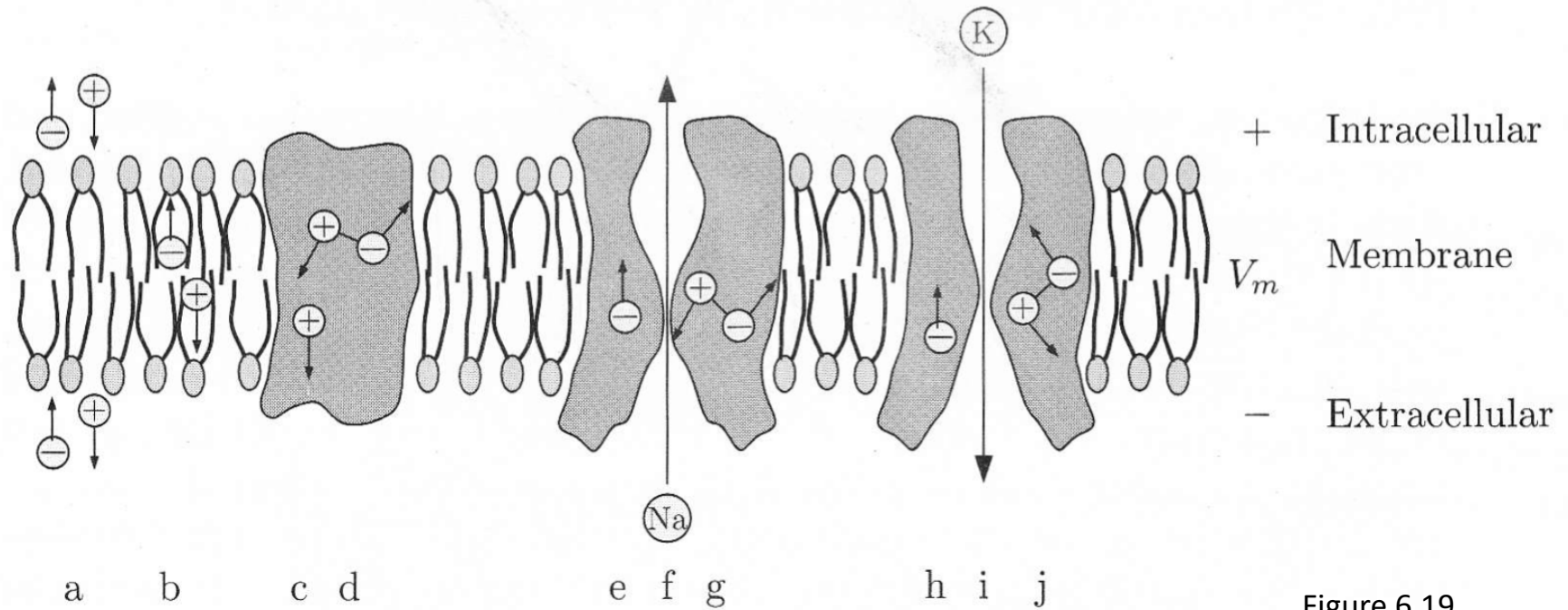


Figure 6.19

- **f, i – Ionic currents** (due to charge “flow” across membrane)
- **a-e, g, h, j – Capacitive currents** (due to charge “displacement” or redistribution along/inside membrane)

Gating current

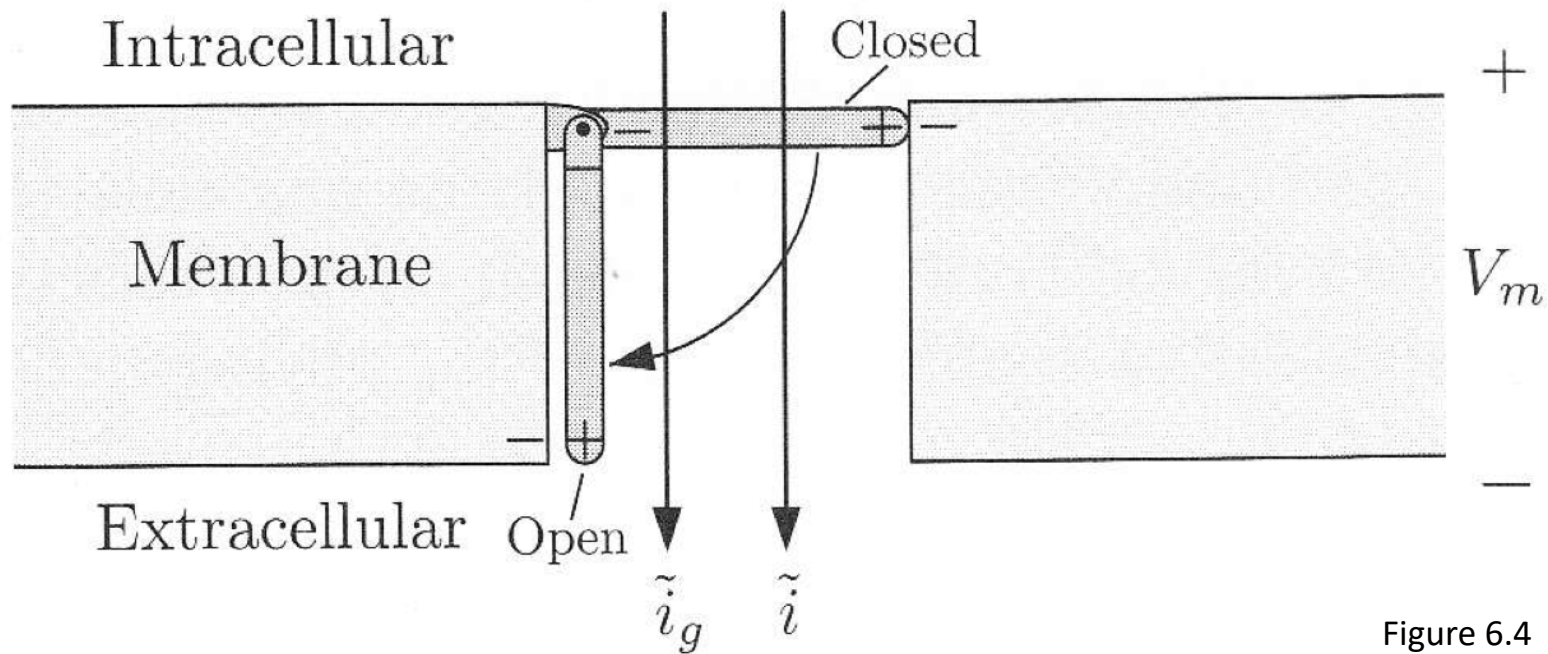


Figure 6.4

- Component (i_g) of the capacitive current
- Due to channel (molecule with non-uniform charge distribution) moving open/closed

Separating Out the Gating Current

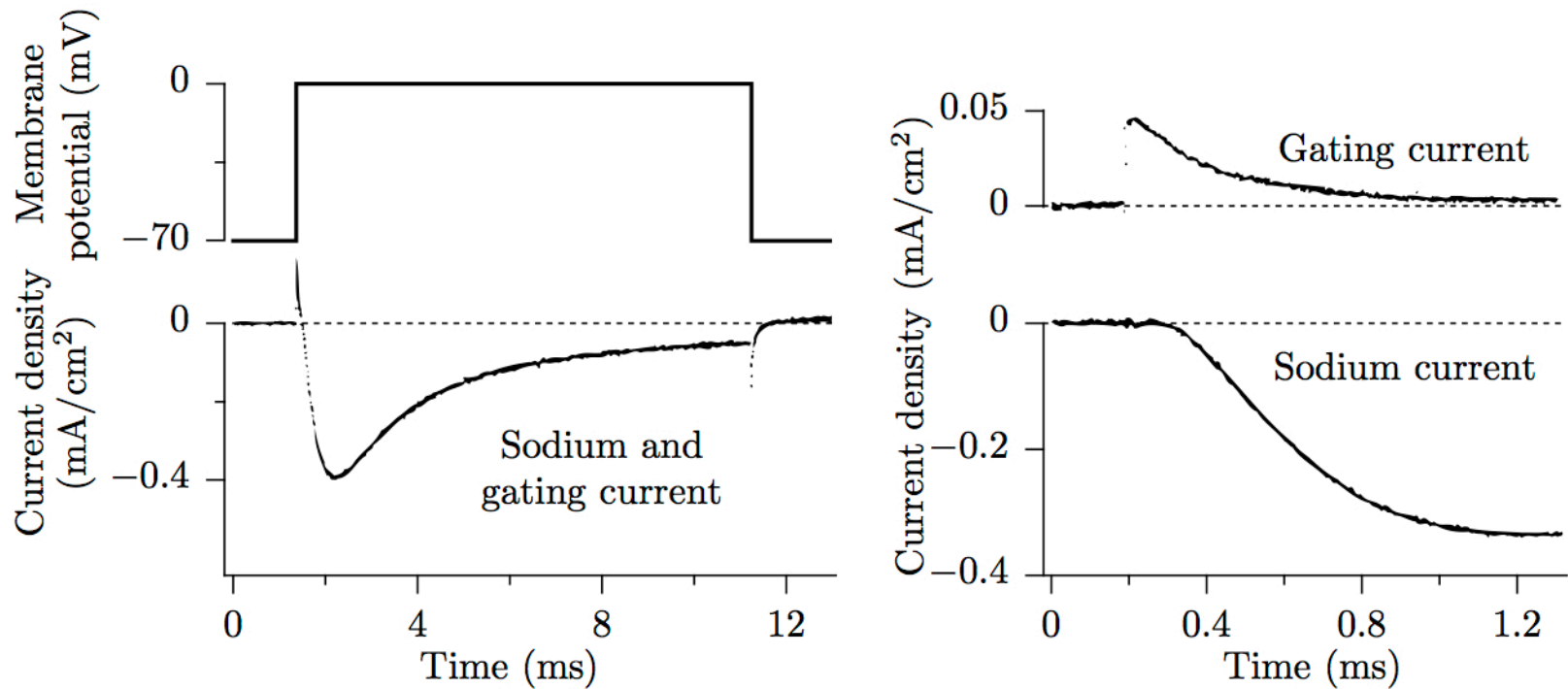
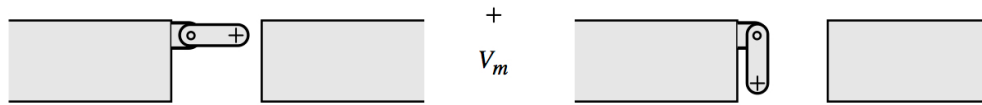
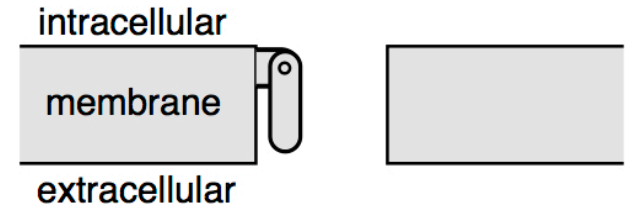
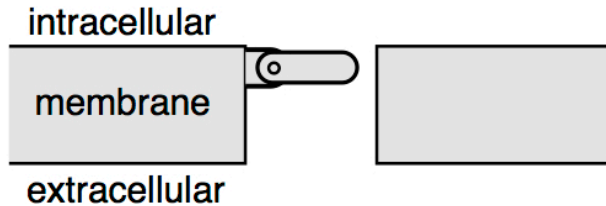


Figure 6.22

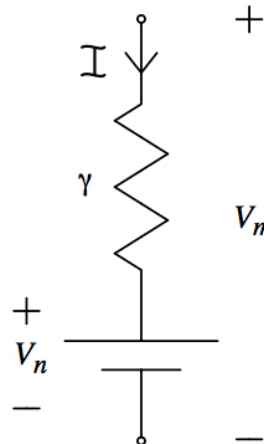
Ion Channel Model: Two Parts

1. Two-state gate model of kinetics



2. Passive electrodiffusive model of permeation

γ = single open-channel conductance



→ For a gate that is either closed or open, conductance is equal to $[0, \gamma]$ respectively

Model: Voltage-Gated Two-State Molecular Gate

Note: The interplay between micro- & macro-scopic descriptions requires a transition into the domain of probability & expectation values

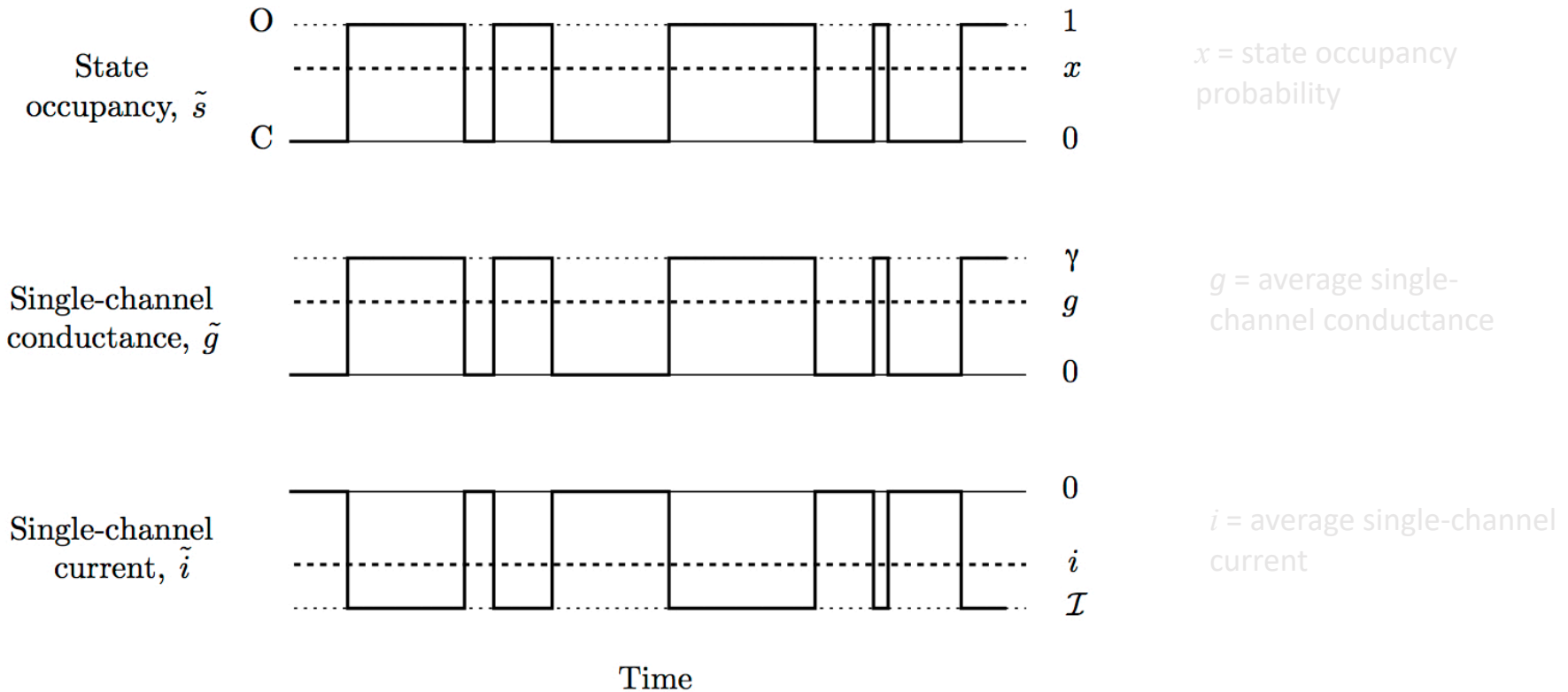
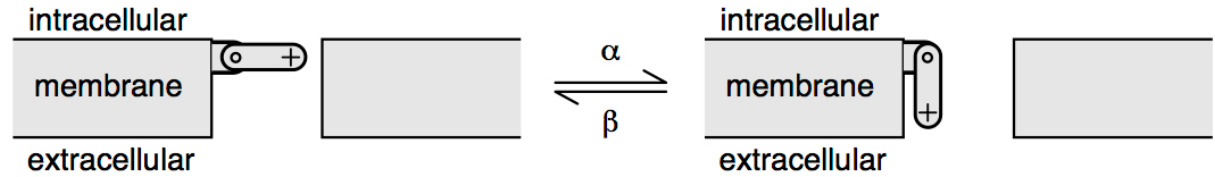
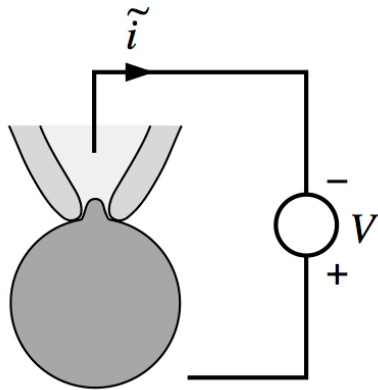
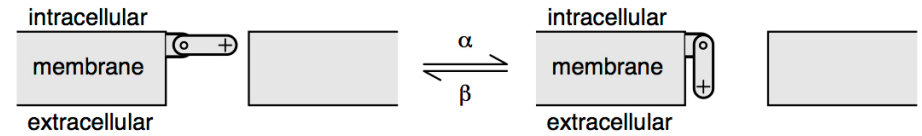


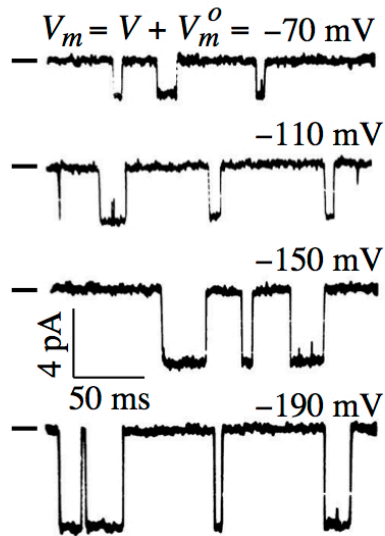
Figure 6.33 (mod)

→ Note stochastic nature for an individual channel

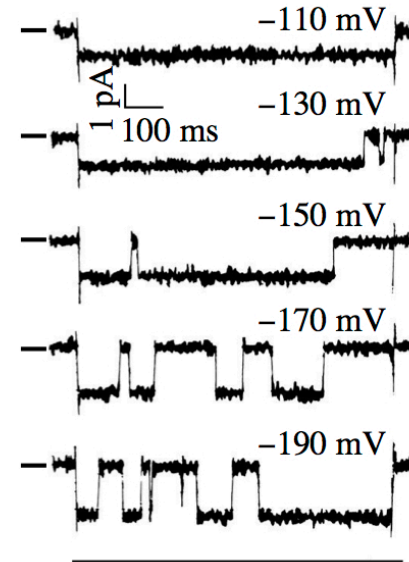
Model: Voltage-Gated Two-State Molecular Gate (*Stochasticity*)



Ligand-gated channel



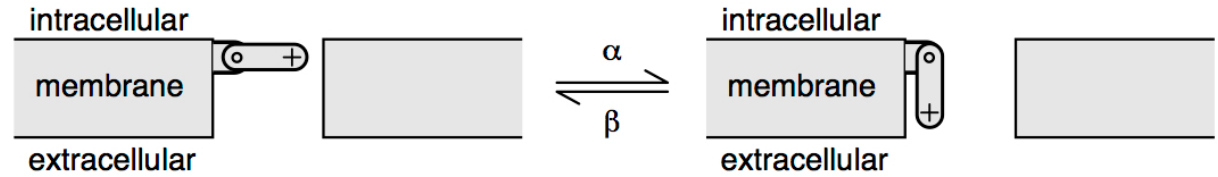
Voltage-gated channel



Why would the state of an individual channel be “stochastic” (i.e., randomly fluctuating)?

→ Molecular size + thermodynamics

Model: Voltage-Gated Two-State Molecular Gate (*Expected Values*)



Assume \mathcal{N} channels per unit area, of which $n(t)$ are open.

$n(t)$ is average # of open channels

$$\frac{dn(t)}{dt} = \alpha(\mathcal{N} - n(t)) - \beta n(t)$$

$$n(t) = n_{\infty} + (n(0) - n_{\infty}) e^{-t/\tau_x}; \quad n_{\infty} = \frac{\alpha}{\alpha + \beta} \mathcal{N}, \quad \tau_x = \frac{1}{\alpha + \beta}$$

Assume \mathcal{N} is large.

$$x(t) = \text{probability gate is open} \approx \frac{n(t)}{\mathcal{N}}$$

$$x(t) = x_{\infty} + (x(0) - x_{\infty}) e^{-t/\tau_x}; \quad x_{\infty} = \frac{\alpha}{\alpha + \beta}, \quad \tau_x = \frac{1}{\alpha + \beta}$$

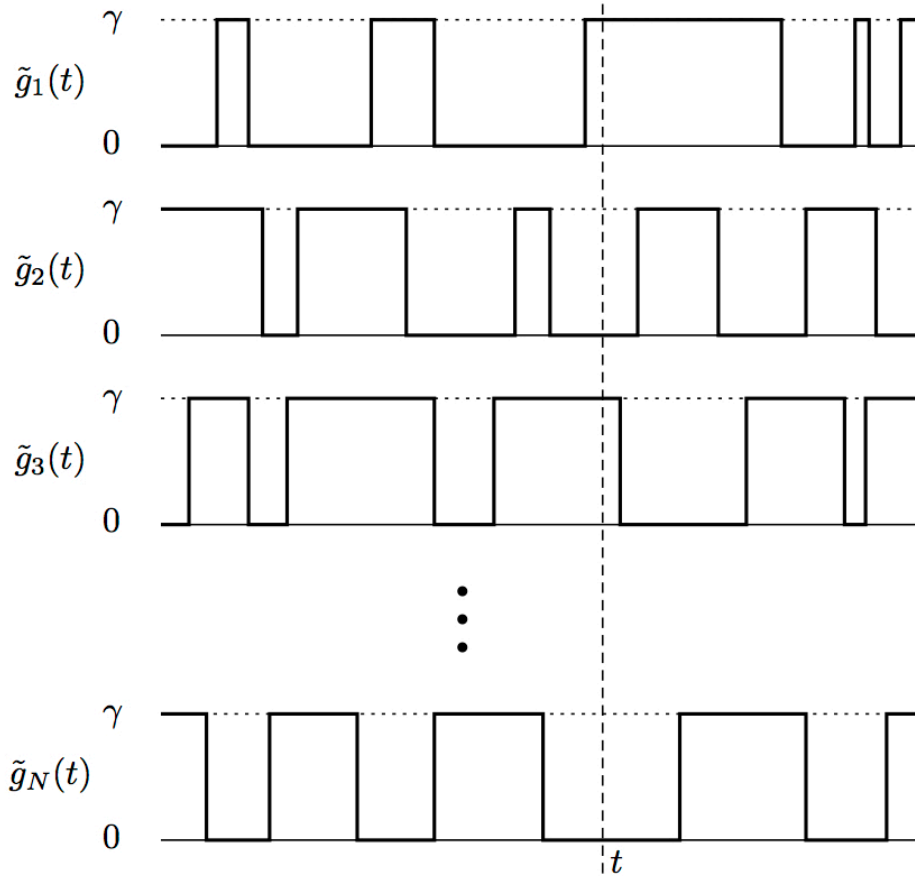


Figure 6.34

→ Microscopic model (+ law of large numbers) gives rise to macroscopic behavior

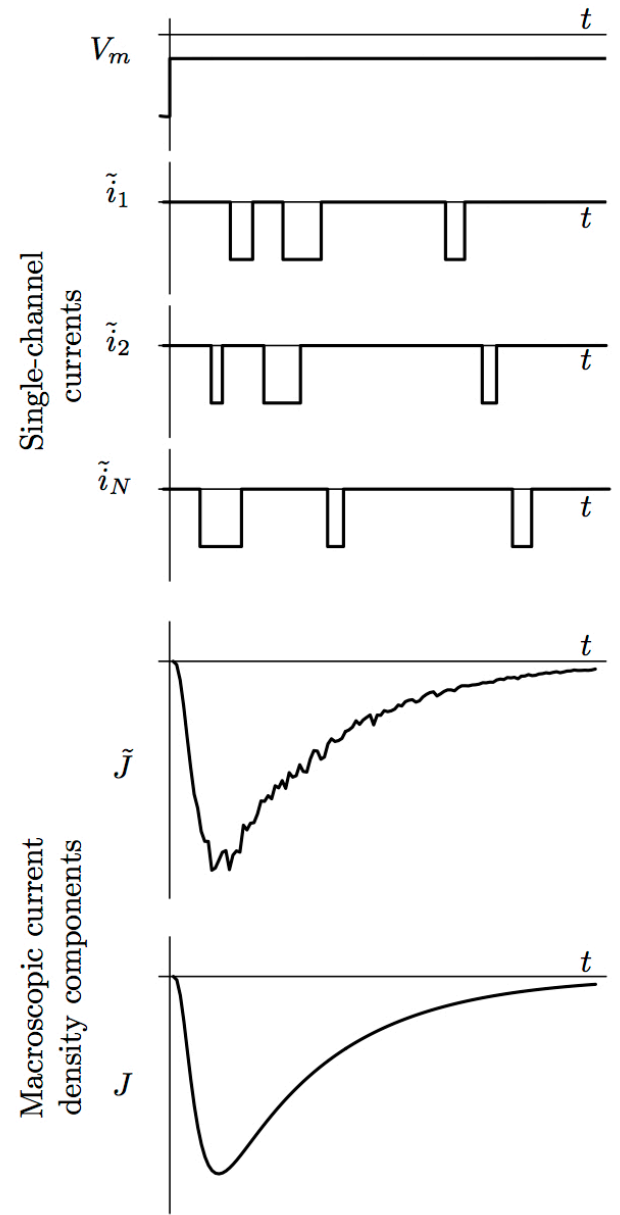


Figure 6.50 (mod)

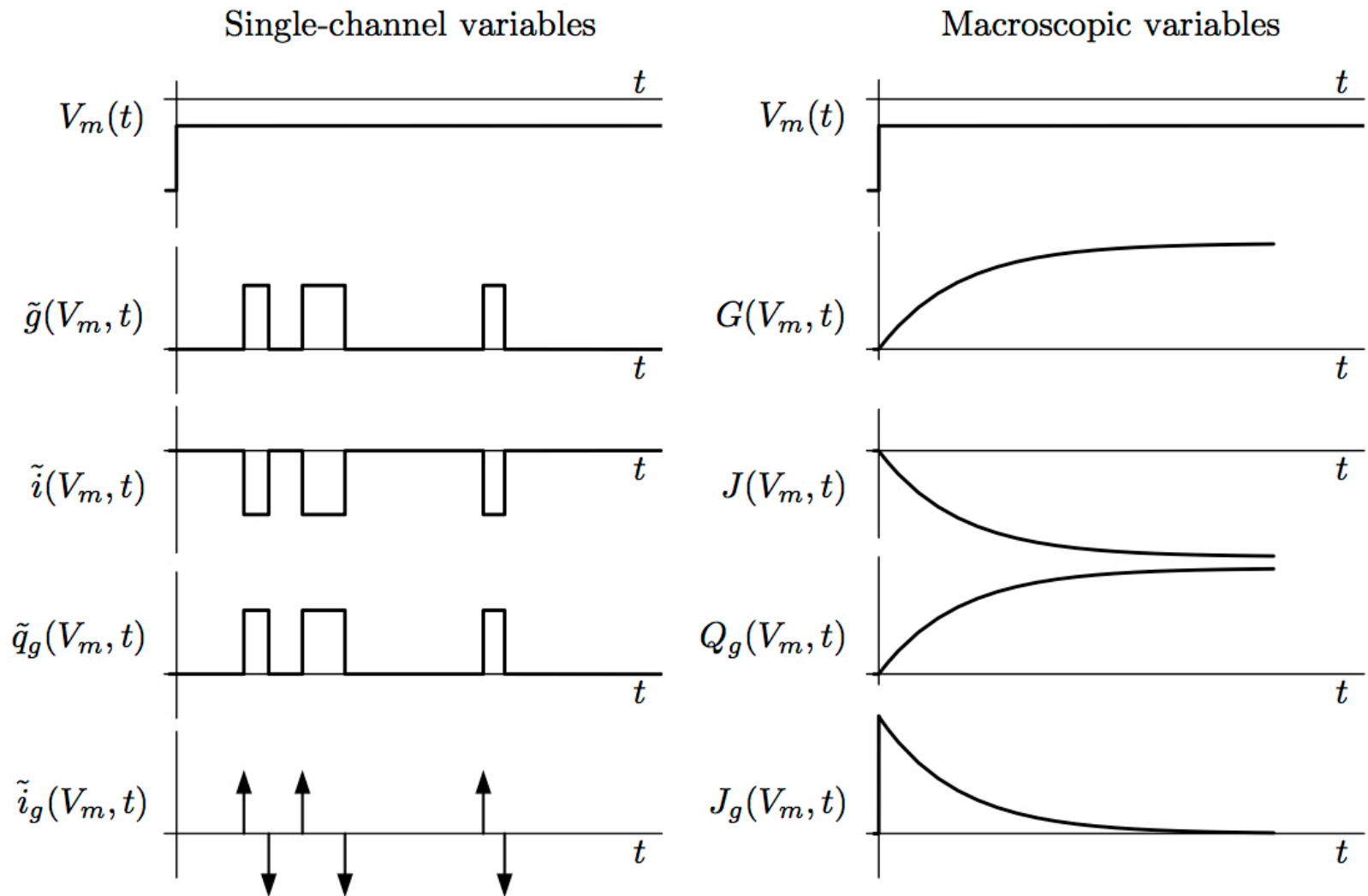


Figure 6.52

Biophysically, this figure encapsulates numerous key ideas....

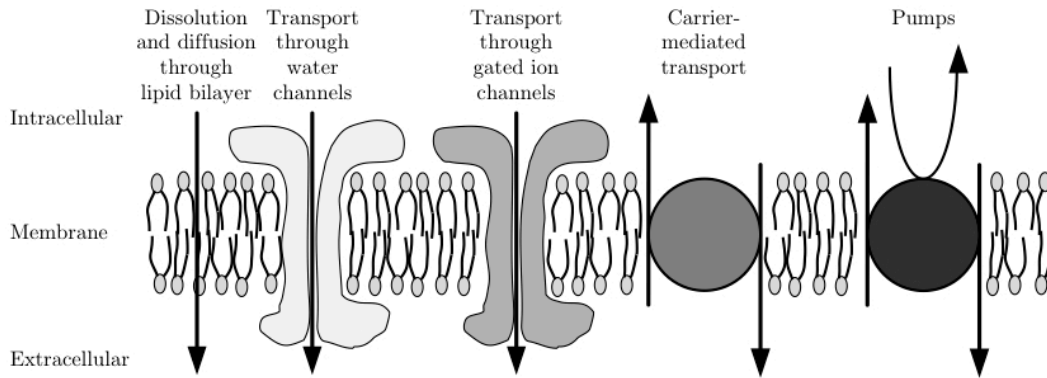


Figure 2.19

$$G_K(V_m, t) = \bar{G}_K n^4(V_m, t)$$

$$G_{Na}(V_m, t) = \bar{G}_{Na} m^3(V_m, t) h(V_m, t)$$

$$n(V_m, t) + \tau_n(V_m) \frac{dn(V_m, t)}{dt} = n_\infty(V_m)$$

$$m(V_m, t) + \tau_m(V_m) \frac{dm(V_m, t)}{dt} = m_\infty(V_m)$$

$$h(V_m, t) + \tau_h(V_m) \frac{dh(V_m, t)}{dt} = h_\infty(V_m)$$

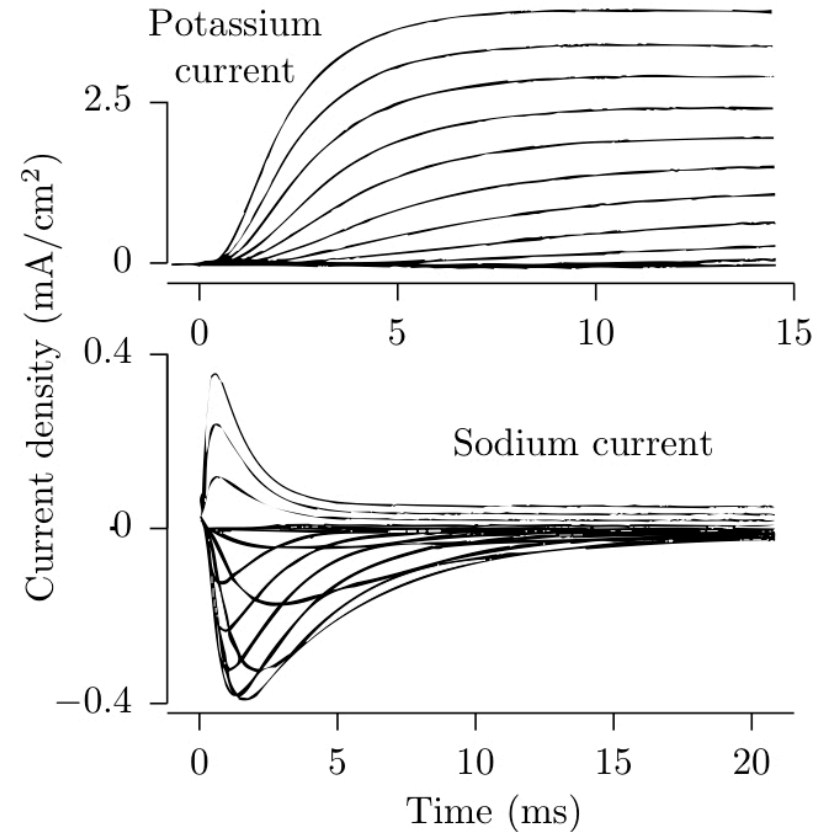


Figure 4.20

Question:

So what do m , h , and n physically represent?

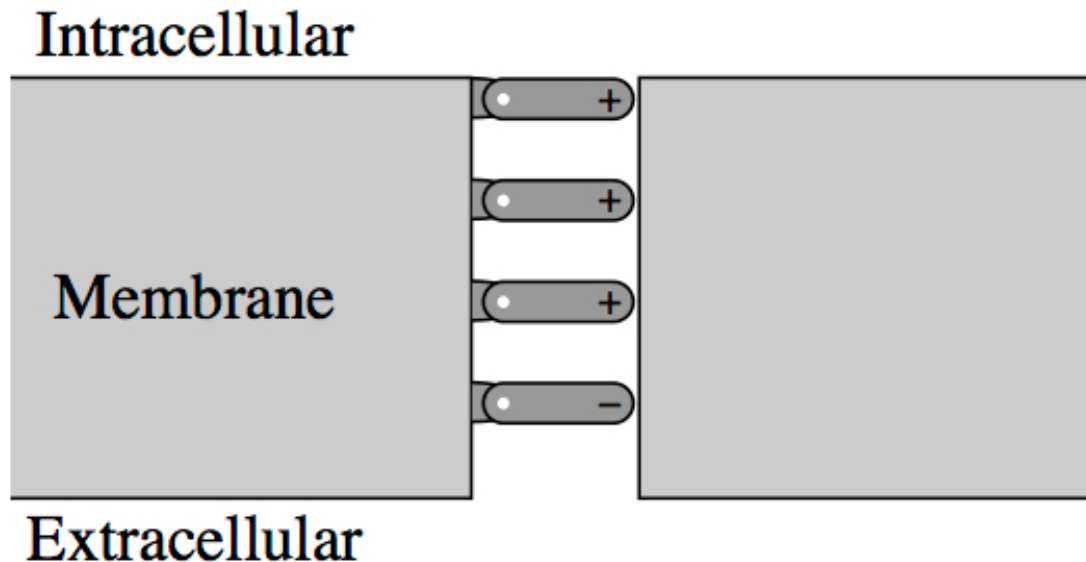
$$G_K(V_m, t) = \bar{G}_K n^4(V_m, t)$$

$$G_{Na}(V_m, t) = \bar{G}_{Na} m^3(V_m, t) h(V_m, t)$$

$$n(V_m, t) + \tau_n(V_m) \frac{dn(V_m, t)}{dt} = n_\infty(V_m)$$

$$m(V_m, t) + \tau_m(V_m) \frac{dm(V_m, t)}{dt} = m_\infty(V_m)$$

$$h(V_m, t) + \tau_h(V_m) \frac{dh(V_m, t)}{dt} = h_\infty(V_m)$$



Exercises

State whether each of the following is true or false, and give a reason for your answer.

- a. Tetrodotoxin blocks the flow of potassium through the sodium channel.
- b. The macroscopic sodium current recorded by an electrode in a cell is a sum of the single-channel sodium currents that flow through single sodium channels.
- c. The macroscopic sodium current recorded by an electrode in a cell is the average of the single-channel sodium currents that flow through single sodium channels.
- d. Ionic and gating currents give identical information about channel kinetic properties.

Exercises

Figure 6.72 shows two putative records of membrane currents recorded from two membrane patches, each of which contains a single channel, in response to a step of depolarizing membrane potential. Each of these channels has a linear voltage-current characteristic when the channel is open.

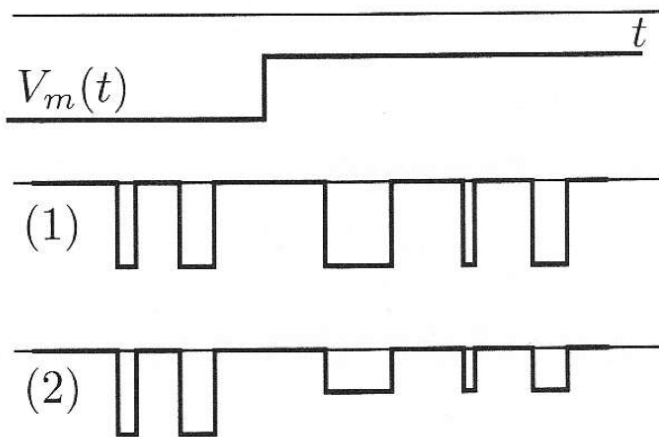


Figure 6.72 Two putative single-channel currents in response to a voltage step (Exercise 6.5).

- Which, if any, of these records could be from a single voltage-gated channel? Explain.
- Which, if any, of these records could be from a single channel that is not voltage gated? Explain.

Exercises (SOL)

State whether each of the following is true or false, and give a reason for your answer.

- a. Tetrodotoxin blocks the flow of potassium through the sodium channel.
- b. The macroscopic sodium current recorded by an electrode in a cell is a sum of the single-channel sodium currents that flow through single sodium channels.
- c. The macroscopic sodium current recorded by an electrode in a cell is the average of the single-channel sodium currents that flow through single sodium channels.
- d. Ionic and gating currents give identical information about channel kinetic properties.

Exercise 6.4

- a. **True.** Tetrodotoxin blocks the sodium channel. Hence, it blocks the flow of any ion that can pass through the channel including potassium
- b. **True.**
- c. **False.** See part b.
- d. **False.** Gating currents give information about charge movements in the membrane between any states — conducting and non-conducting states — whereas ionic current give information about the conducting states only.

Exercises (SOL)

Exercise 6.5 Trace 1 shows a single-channel current with two states of conduction: one current is zero and the other is negative. The negative current represents ion flow when the channel is open. The magnitude of that current is not changed by the step change in membrane potential. This is inconsistent with the assumption that the open-channel voltage-current relation is linear. Therefore trace 1 cannot result from an ion channel: neither from a voltage-gated ion channel nor any other ion channel.

The open-channel currents in trace 2 are different before and after the step change in membrane potential. This is expected if the open-channel voltage-current relation is linear. From this short segment of data, one cannot conclude that the probability that the channel is open has or has not changed during the step change in membrane potential. Therefore, the current in trace 2 could be from a voltage-gated ion channel or any other ion channel.

a. Trace 2 only.

b. Trace 2 only.

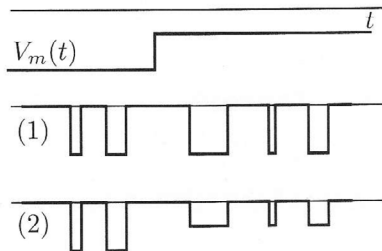


Figure 6.72 Two putative single-channel currents in response to a voltage step (Exercise 6.5).

- Which, if any, of these records could be from a single voltage-gated channel? Explain.
- Which, if any, of these records could be from a single channel that is not voltage gated? Explain.

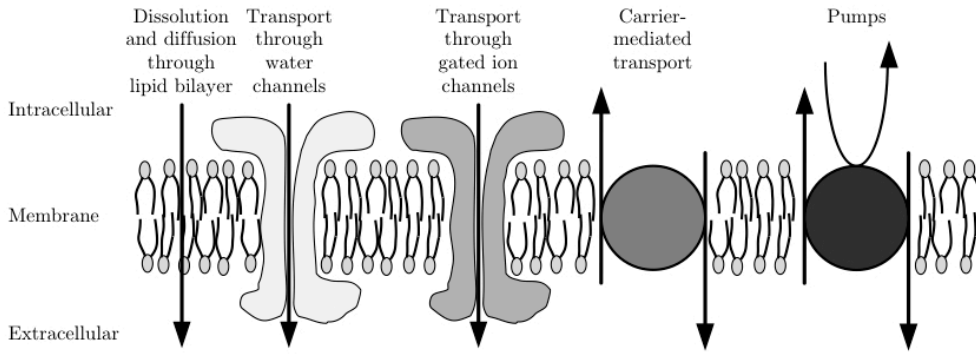
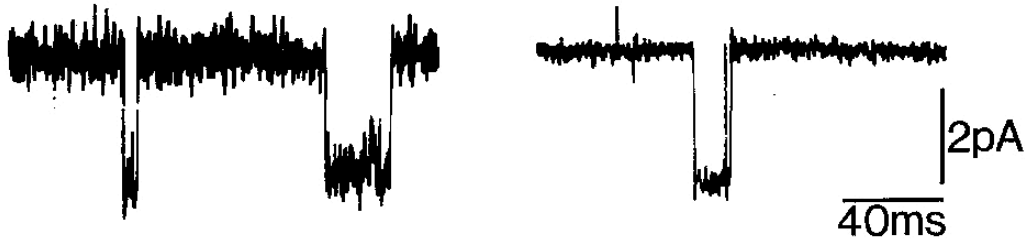
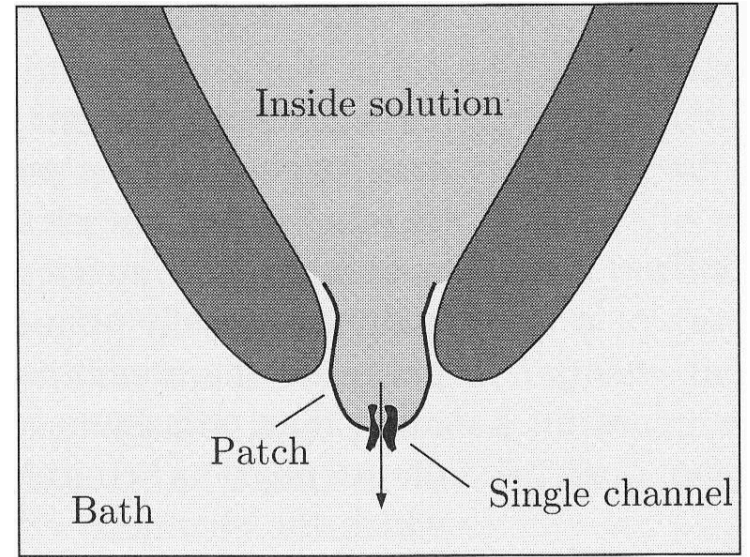


Figure 2.19



Macroscopic sodium current

Single-channel sodium current candidates

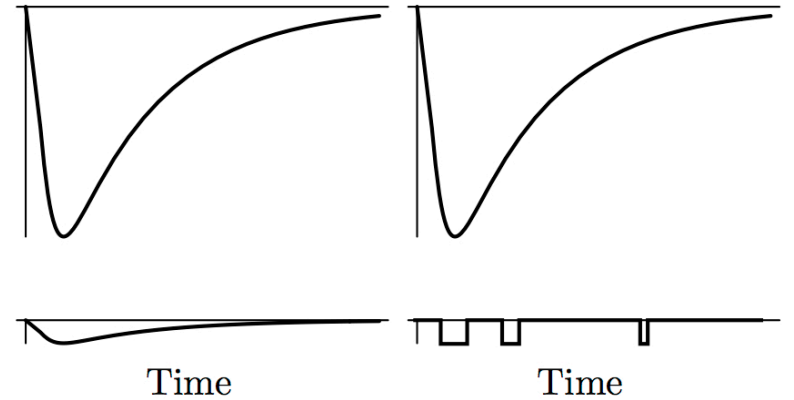


Figure 6.27

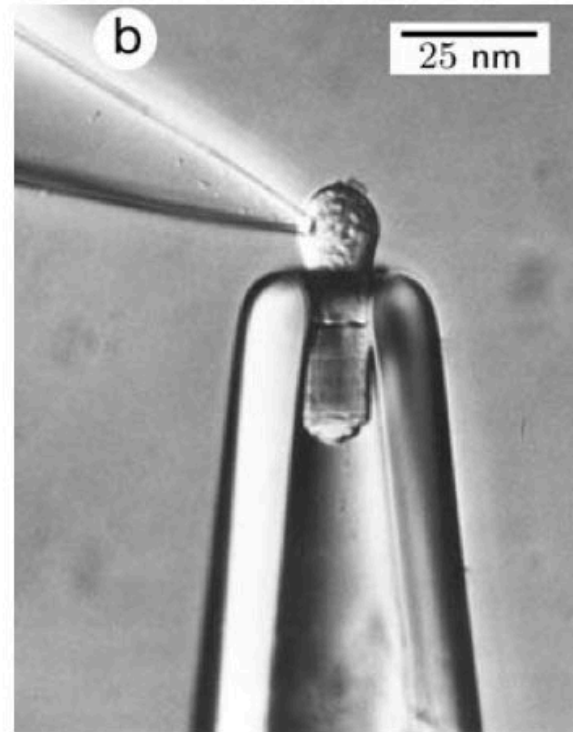
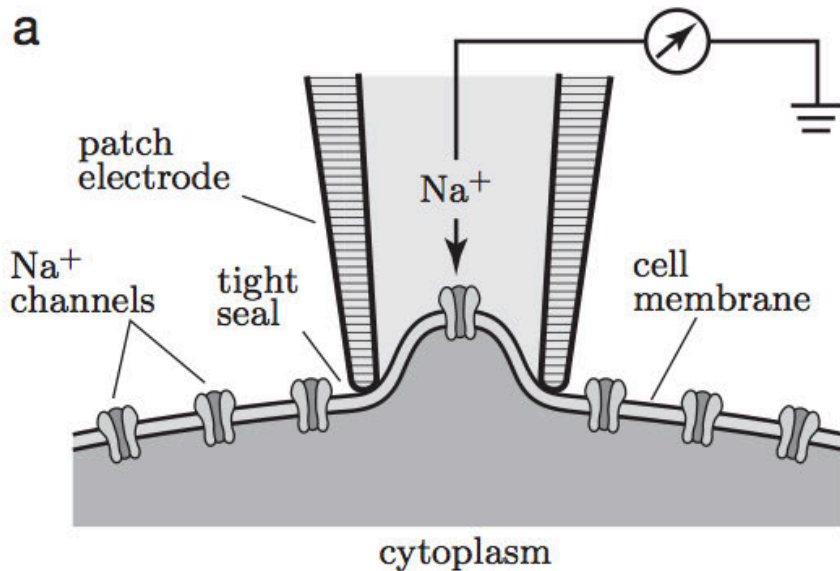


Figure 12.14: (Schematic; optical micrograph.) (a) A small patch of membrane containing only a single voltage-gated sodium channel (or a few) is electrically isolated from the rest of the cell by a patch electrode. The current entering the cell through these channels is recorded by a monitor connected to the patch electrode. (b) Patch-clamp manipulation of a single, live photoreceptor cell from the retina of a salamander. The cell is secured by partially sucking it into a glass micropipette (bottom), while the patch-clamp electrode (upper left) is sealed against a small patch of the cell's plasma membrane. [Digital image kindly supplied by T. D. Lamb; see Lamb et al., 1986.]

Model: Voltage-Gated Two-State Molecular Gate

Note: The interplay between micro- & macro-scopic descriptions requires a transition into the domain of probability & expectation values

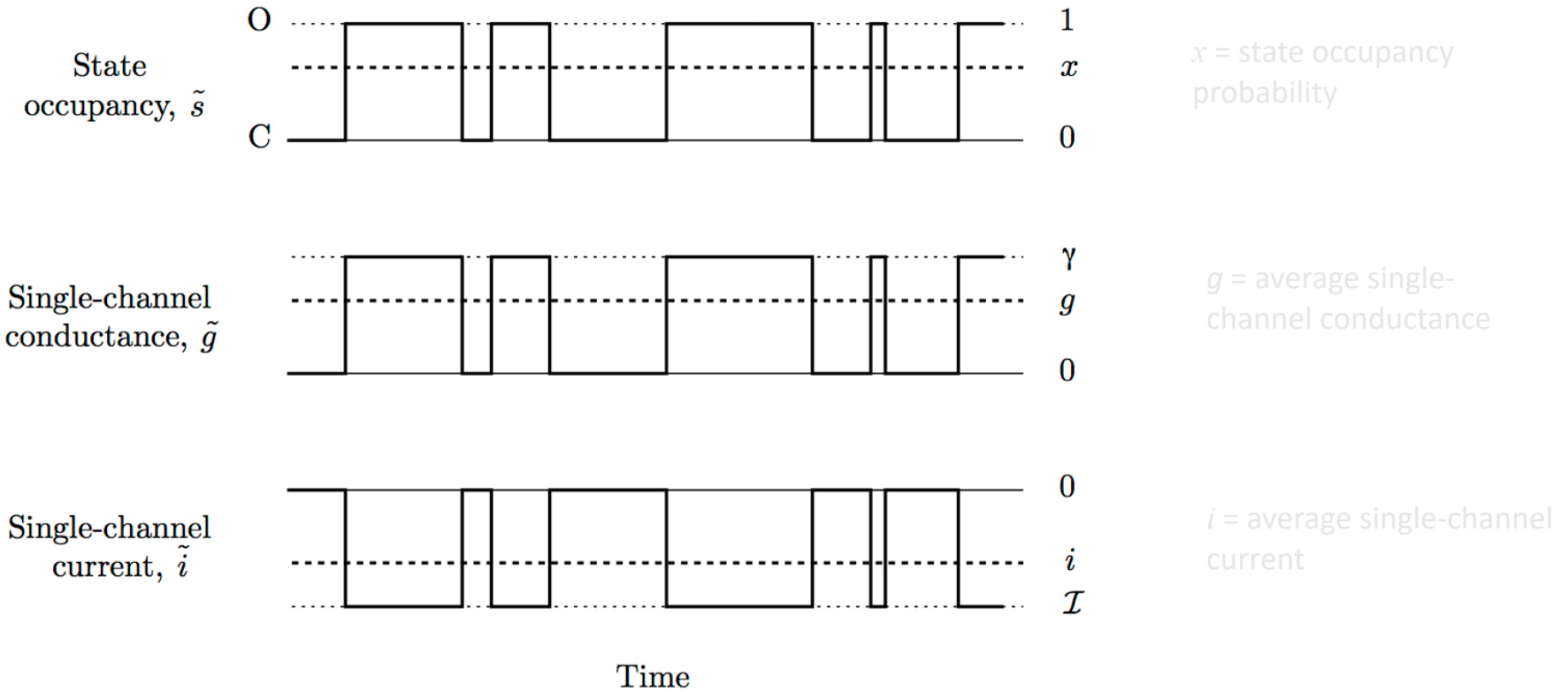
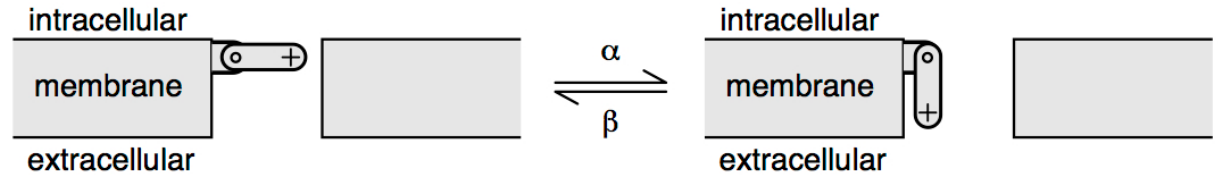


Figure 6.33 (mod)

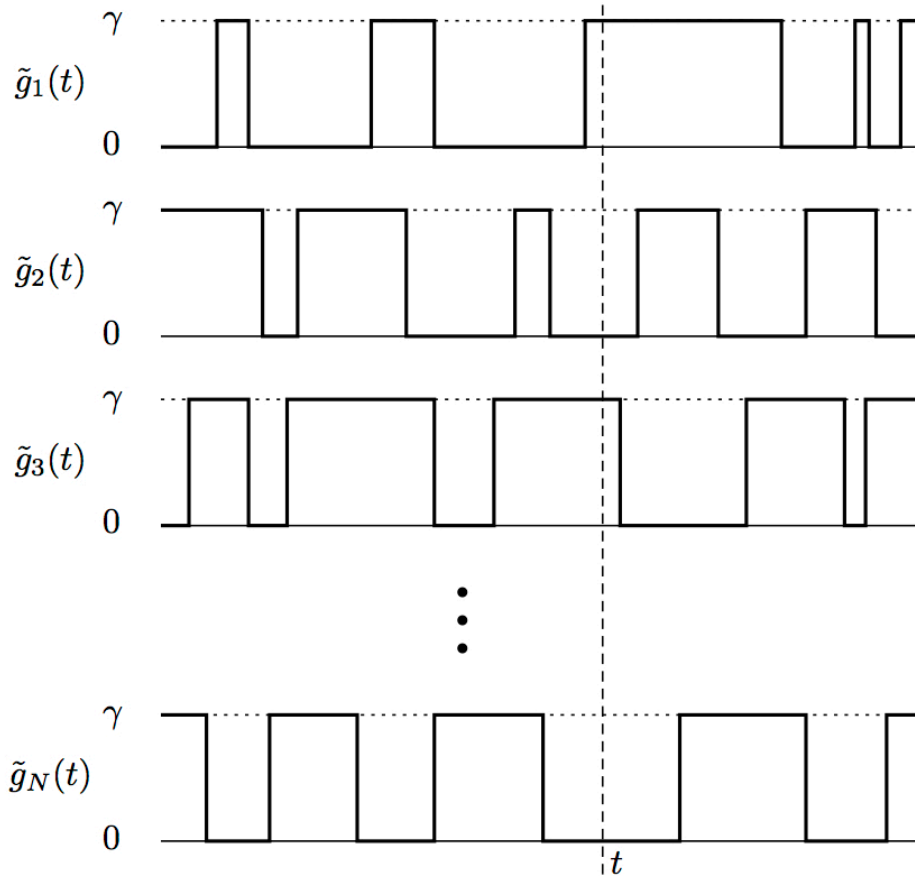


Figure 6.34

→ Microscopic model (+ law of large numbers) gives rise to macroscopic behavior

Question(s): How big must N be? How “local” does it need to be (i.e., as a channel density)?

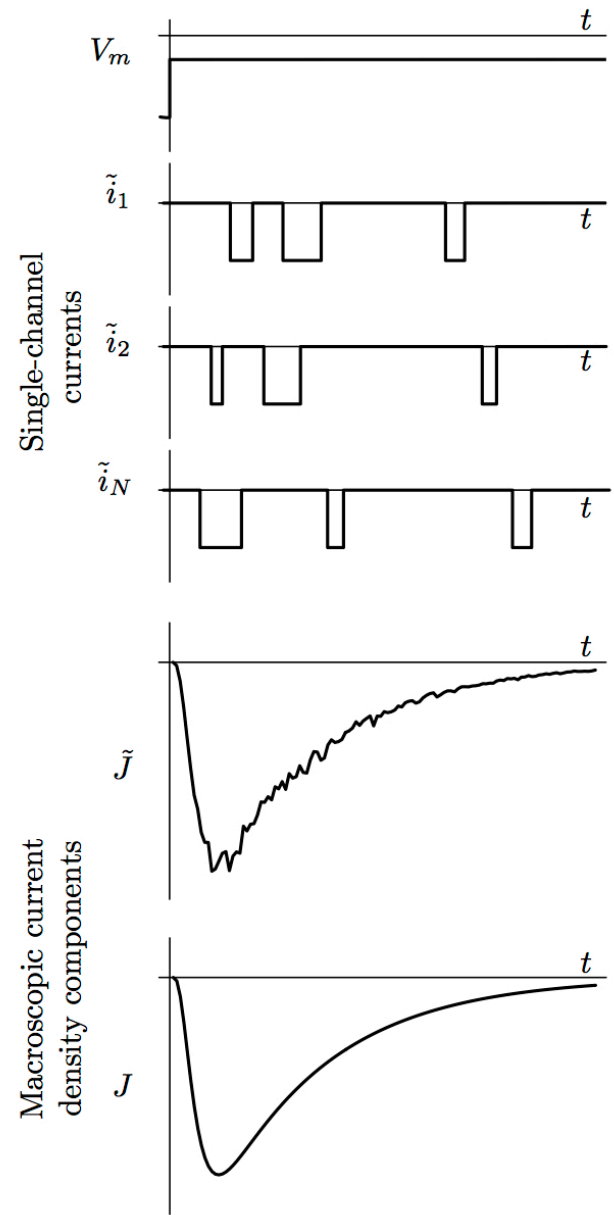
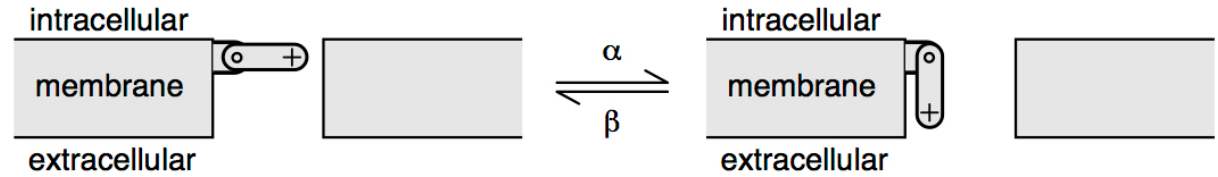


Figure 6.50 (mod)

Model: Voltage-Gated Two-State Molecular Gate (*Expected Values*)



Assume \mathcal{N} channels per unit area, of which $n(t)$ are open.

$n(t)$ is average # of open channels

$$\frac{dn(t)}{dt} = \alpha(\mathcal{N} - n(t)) - \beta n(t)$$

$$n(t) = n_{\infty} + (n(0) - n_{\infty}) e^{-t/\tau_x}; \quad n_{\infty} = \frac{\alpha}{\alpha + \beta} \mathcal{N}, \quad \tau_x = \frac{1}{\alpha + \beta}$$

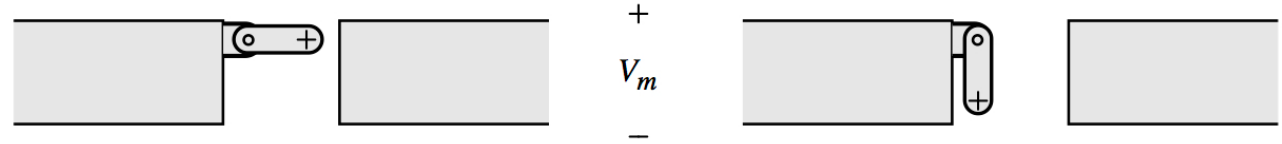
First-order kinetics(!!)

Assume \mathcal{N} is large.

$$x(t) = \text{probability gate is open} \approx \frac{n(t)}{\mathcal{N}}$$

$$x(t) = x_{\infty} + (x(0) - x_{\infty}) e^{-t/\tau_x}; \quad x_{\infty} = \frac{\alpha}{\alpha + \beta}, \quad \tau_x = \frac{1}{\alpha + \beta}$$

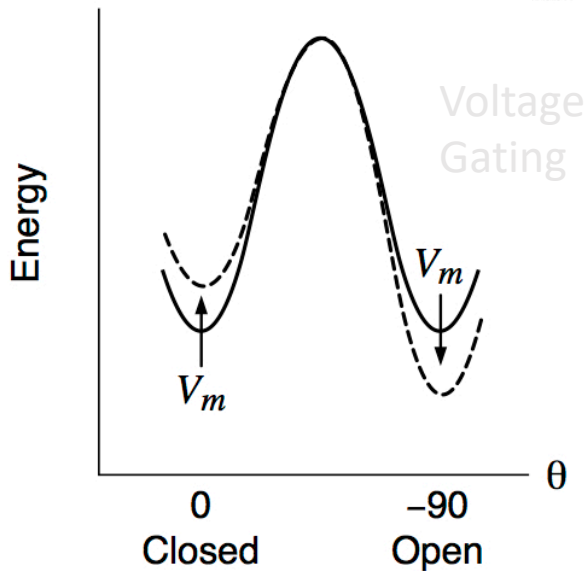
Model: Voltage-Gated Two-State Molecular Gate



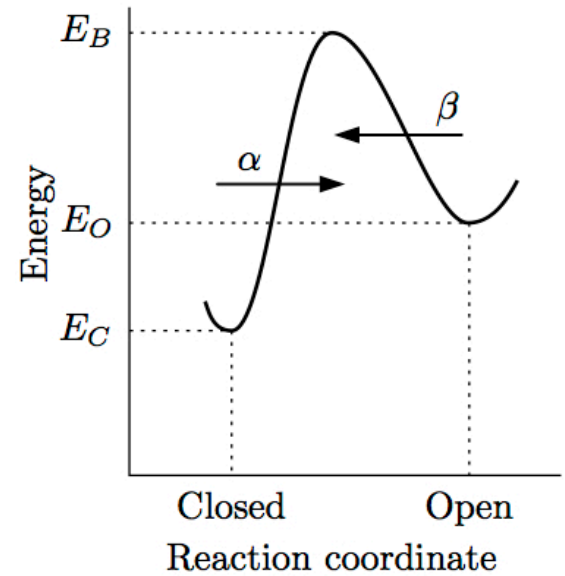
The potential energy of an ion channel includes mechanical, chemical, and electrical contributions, each of which can be different in different conformations. Electrical potential energy depends on both the distribution of charge in the gate and on transmembrane potential. Therefore, E_B , E_O , and E_C depend on V_m .

First-order kinetics variables

$$\frac{dx}{dt} = \alpha_x(1 - x) - \beta_x x$$



→ Potential modifies energy configuration



$$\alpha = Ae^{(E_C - E_B)/kT}$$

$$\beta = Ae^{(E_O - E_B)/kT}$$

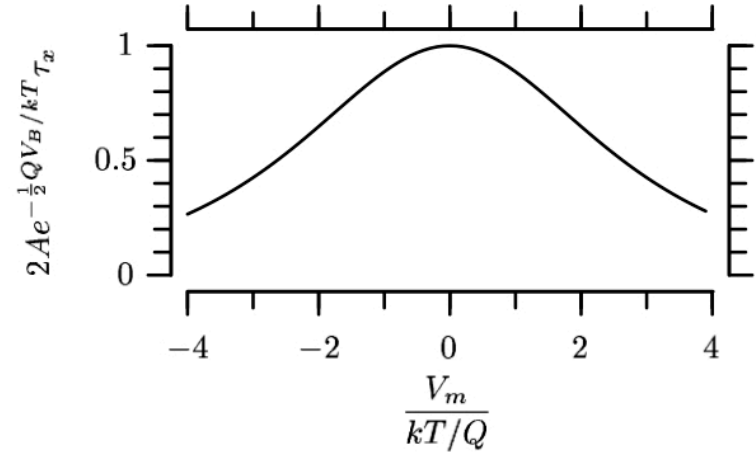
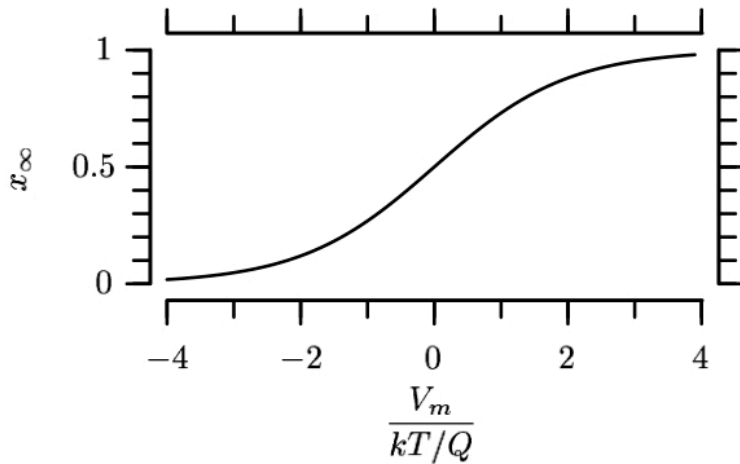
Ex.

$$E_B = \frac{1}{2}QV_B; \quad E_C = \frac{1}{2}QV_m; \quad E_O = -\frac{1}{2}QV_m$$

$$\alpha = A e^{\frac{1}{2}Q(V_m - V_B)/kT}; \quad \beta = A e^{-\frac{1}{2}Q(V_m + V_B)/kT}$$

$$\begin{aligned} \tau_x &= \frac{1}{\alpha + \beta} = \frac{1}{A(e^{\frac{1}{2}Q(V_m - V_B)/kT} + e^{-\frac{1}{2}Q(V_m + V_B)/kT})} \\ &= \frac{1}{Ae^{-\frac{1}{2}QV_B/kT}(e^{\frac{1}{2}QV_m/kT} + e^{-\frac{1}{2}QV_m/kT})} \end{aligned}$$

$$x_\infty = \frac{\alpha}{\alpha + \beta} = \frac{1}{1 + \beta/\alpha} = \frac{1}{1 + e^{-QV_m/kT}}$$



Separating Out the Gating Current

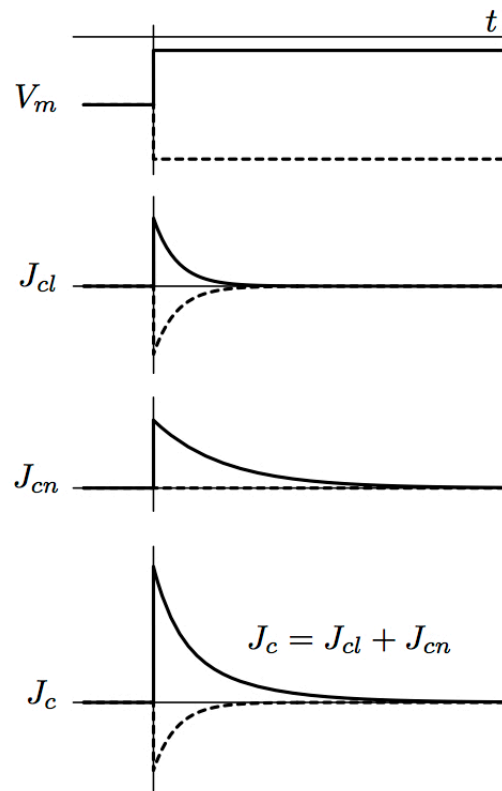
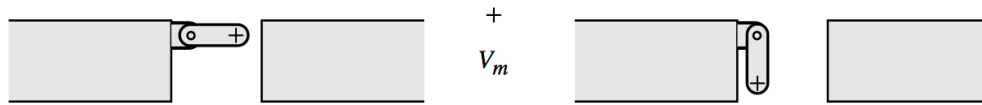


Figure 6.20

Two components (why?)

- Linear
- Nonlinear

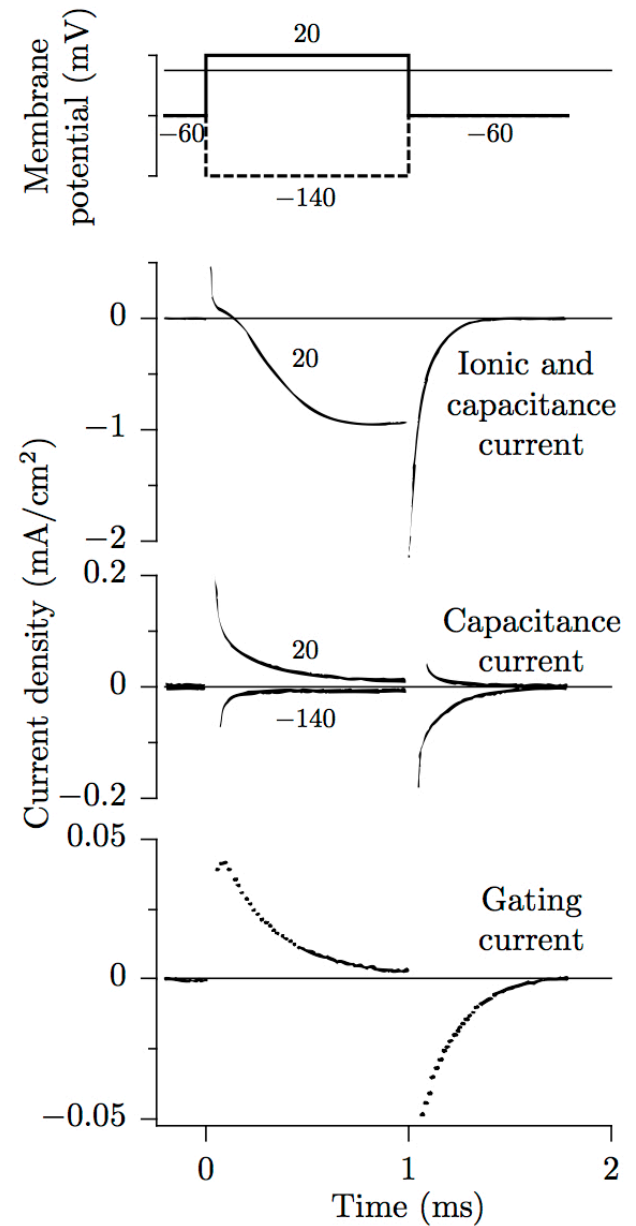
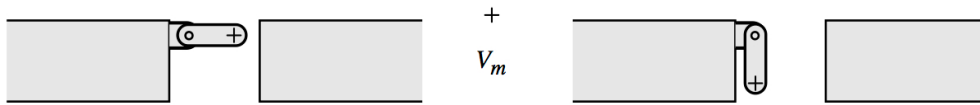


Figure 6.21

Separating Out the Gating Current



→ Sign of gating current can inform about structure/charge distribution of the channel

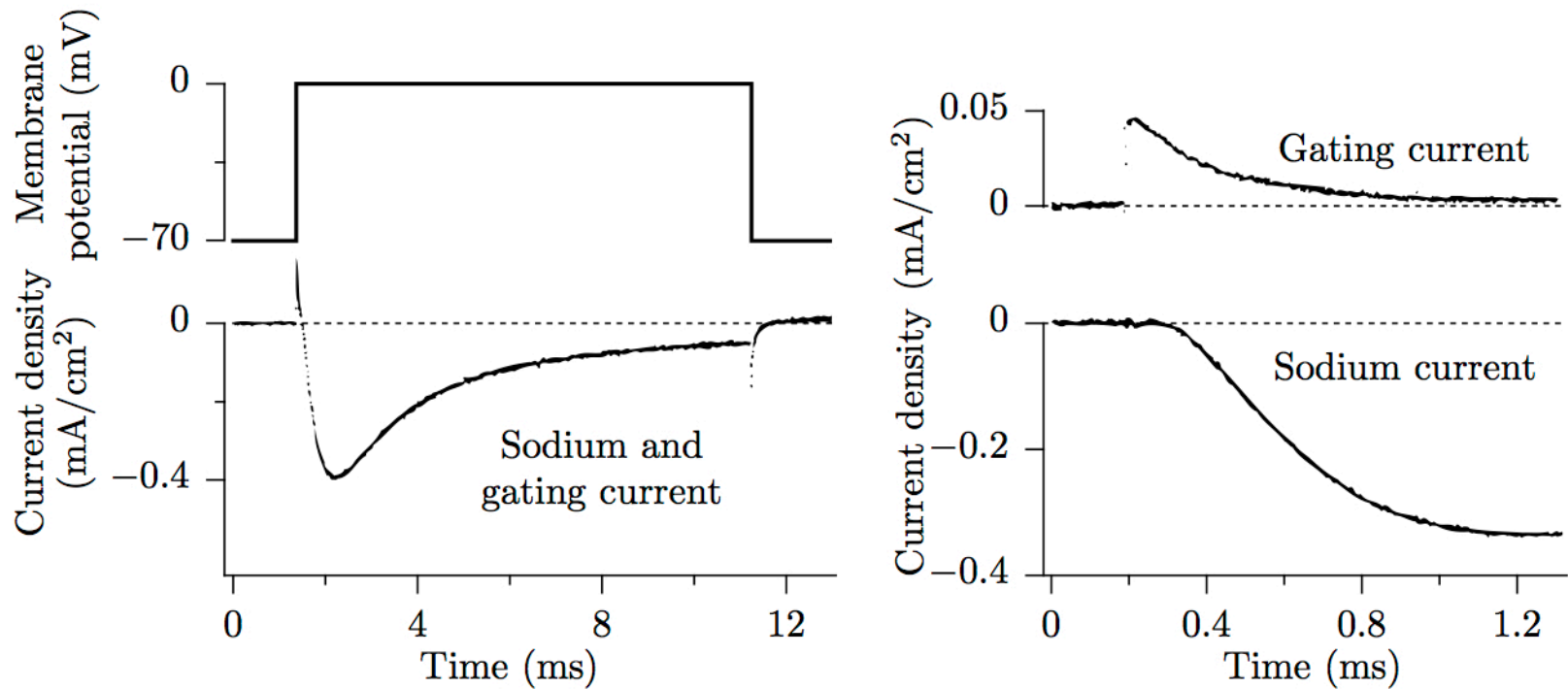


Figure 6.22

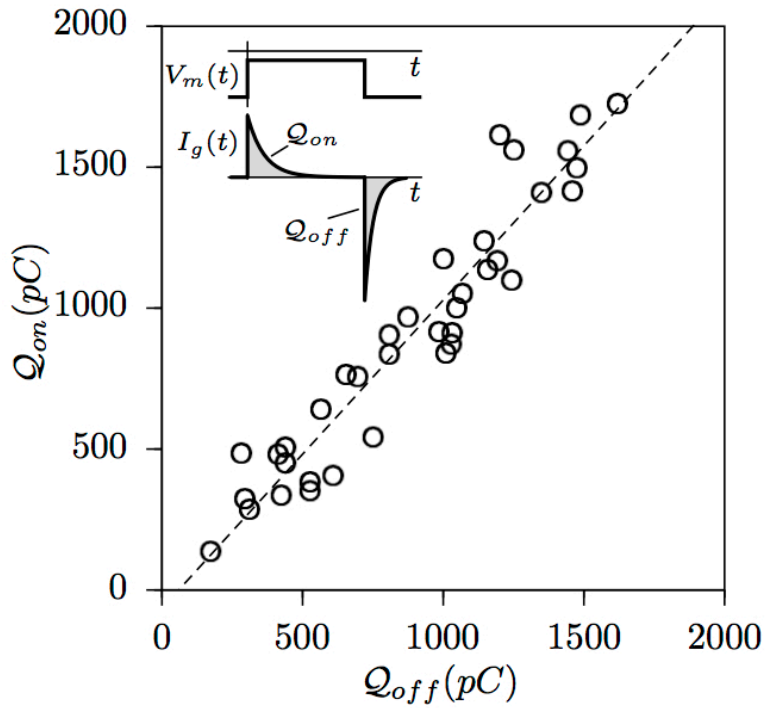


Figure 6.24

Reversibility

(i.e., $Q_{on} = Q_{off}$ implies charge is conserved)

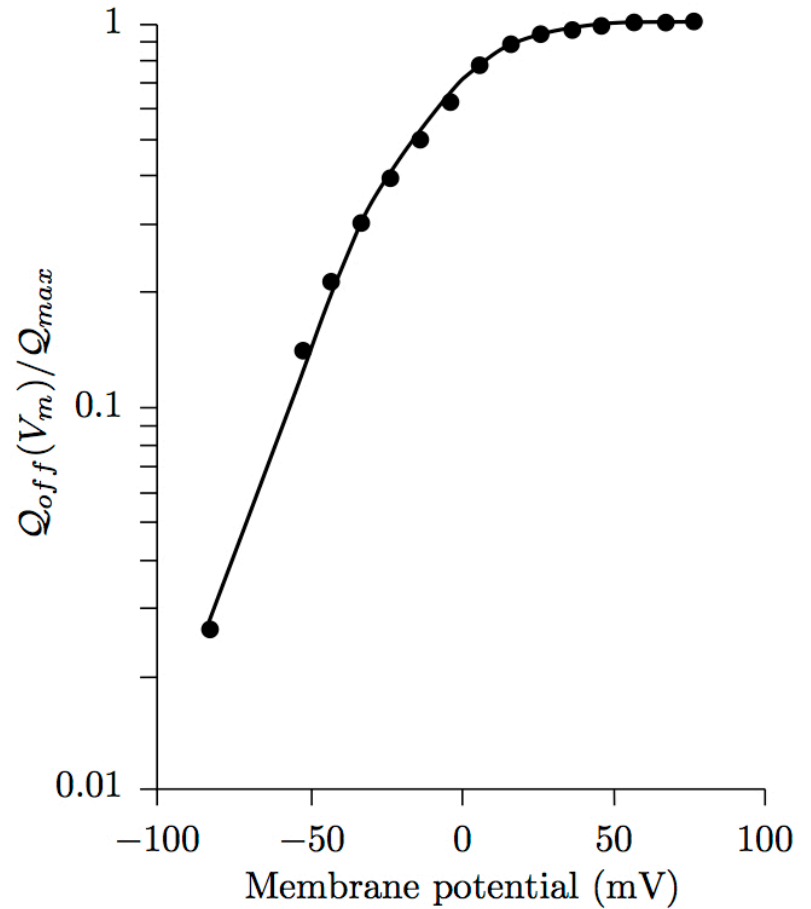


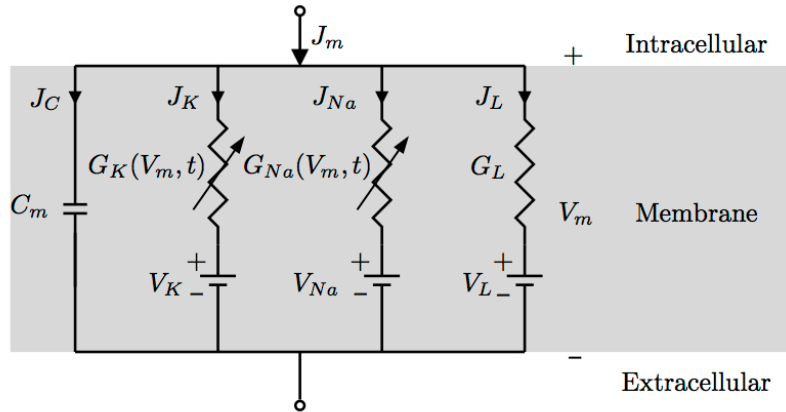
Figure 6.25

Saturation

(i.e., finite number of channels)

Question: If we know the single channel conductance, can we estimate the total # of contributing channels?

Hodgkin Huxley model



$$G_K(V_m, t) = \bar{G}_K n^4(V_m, t)$$

$$G_{Na}(V_m, t) = \bar{G}_{Na} m^3(V_m, t) h(V_m, t)$$

$$n(V_m, t) + \tau_n(V_m) \frac{dn(V_m, t)}{dt} = n_\infty(V_m)$$

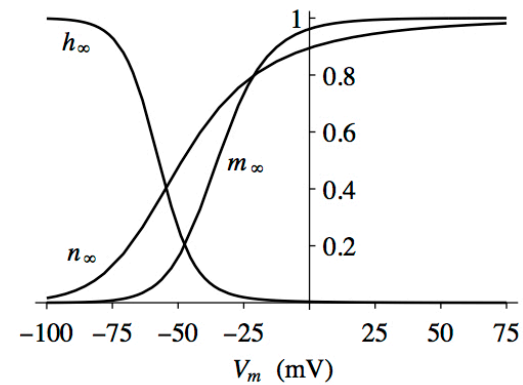
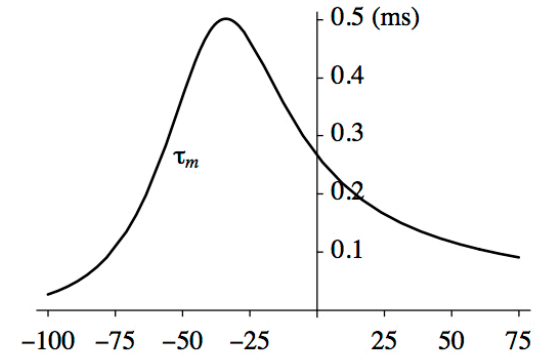
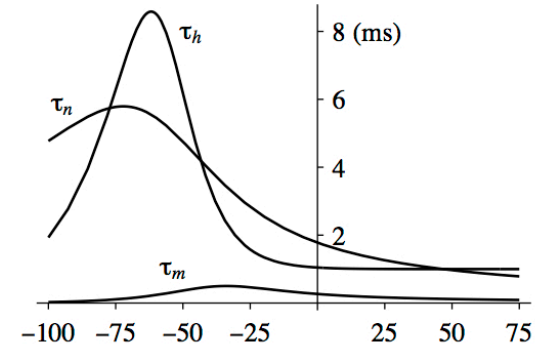
$$m(V_m, t) + \tau_m(V_m) \frac{dm(V_m, t)}{dt} = m_\infty(V_m)$$

$$h(V_m, t) + \tau_h(V_m) \frac{dh(V_m, t)}{dt} = h_\infty(V_m)$$

$$\bar{G}_{Na} = 120, \bar{G}_K = 36, \text{ and } G_L = 0.3 \text{ mS/cm}^2;$$

$$c_{Na}^o = 491, c_{Na}^i = 50, c_K^o = 20.11, c_K^i = 400 \text{ mmol/L};$$

$$C_m = 1 \text{ } \mu\text{F/cm}^2; V_L = -49 \text{ mV}; \text{ temperature is } 6.3^\circ\text{C}.$$



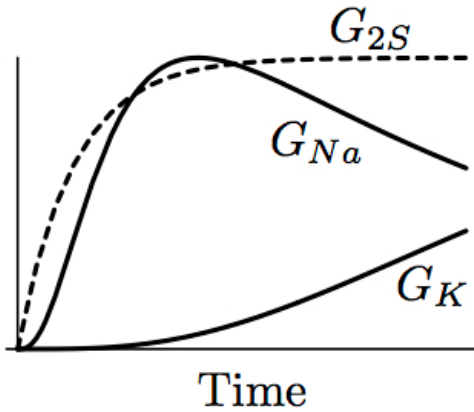
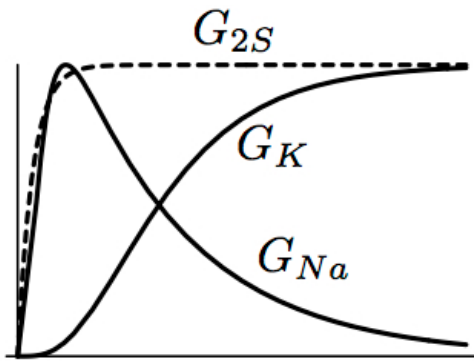


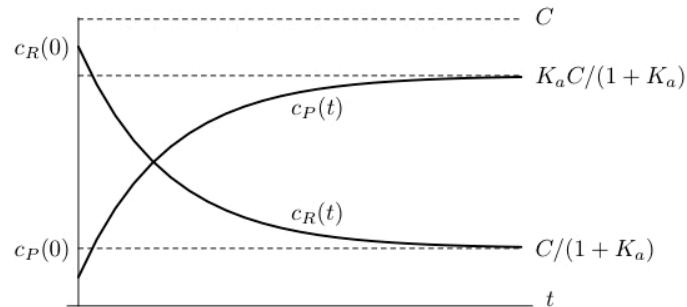
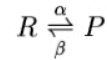
Figure 6.53

Two-state model \rightarrow First-order kinetics

$$\tau_x \frac{dx}{dt} + x = x_\infty \quad \frac{dx}{dt} = \alpha_x(1-x) - \beta_x x$$

$$x_\infty = \alpha_x / (\alpha_x + \beta_x) \text{ and } \tau_x = 1 / (\alpha_x + \beta_x)$$

First-order, reversible reaction

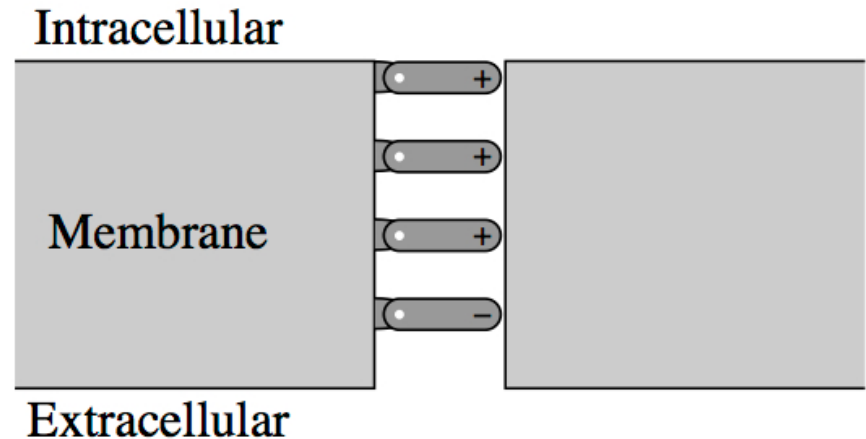


$$\tau = \frac{1}{\alpha + \beta}$$

\rightarrow Single two-state model too 'simple'

$$G_K(V_m, t) = \bar{G}_K n^4(V_m, t)$$

$$G_{Na}(V_m, t) = \bar{G}_{Na} m^3(V_m, t) h(V_m, t)$$



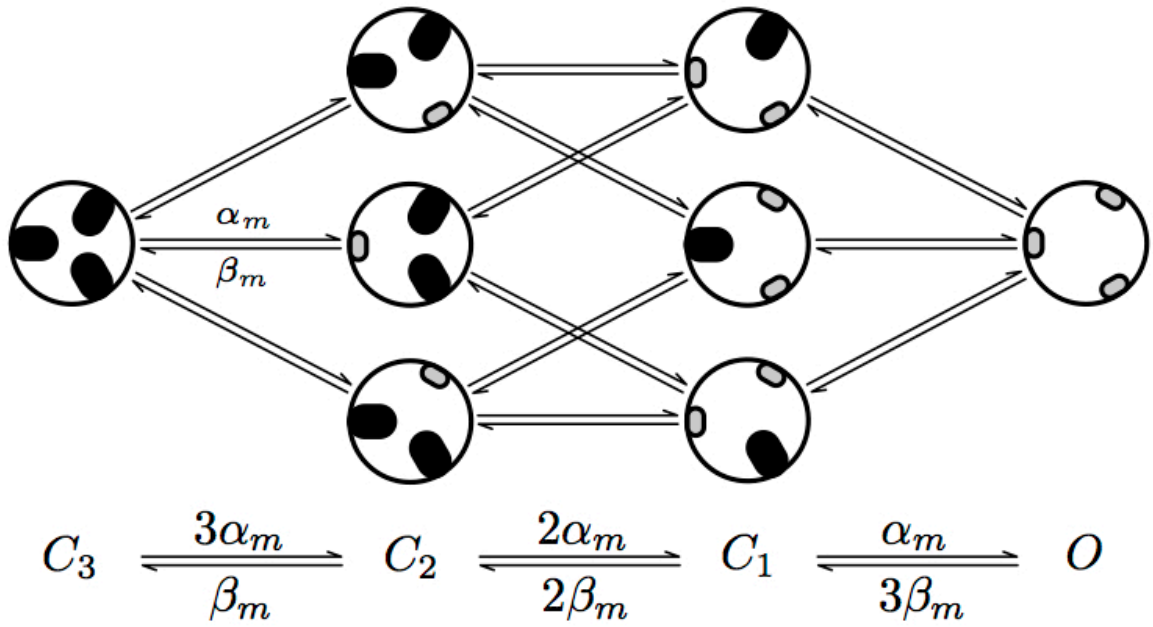
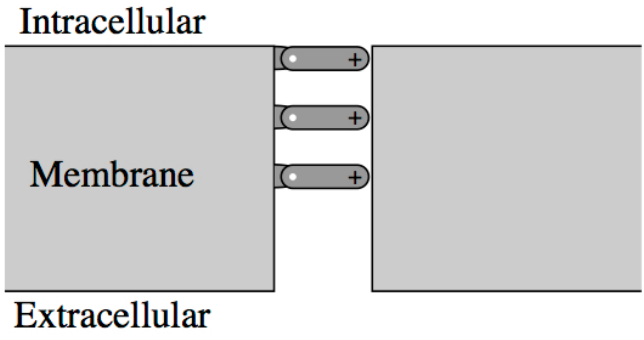


Figure 6.54

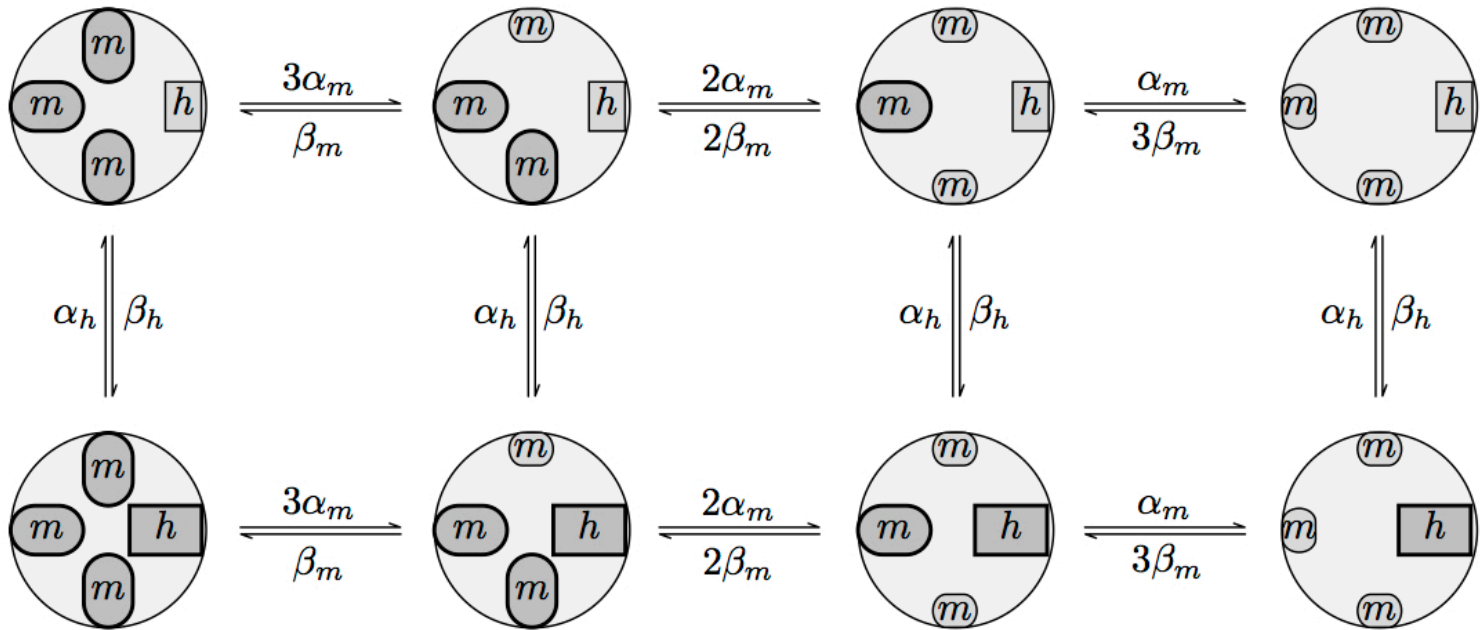


Figure 6.55

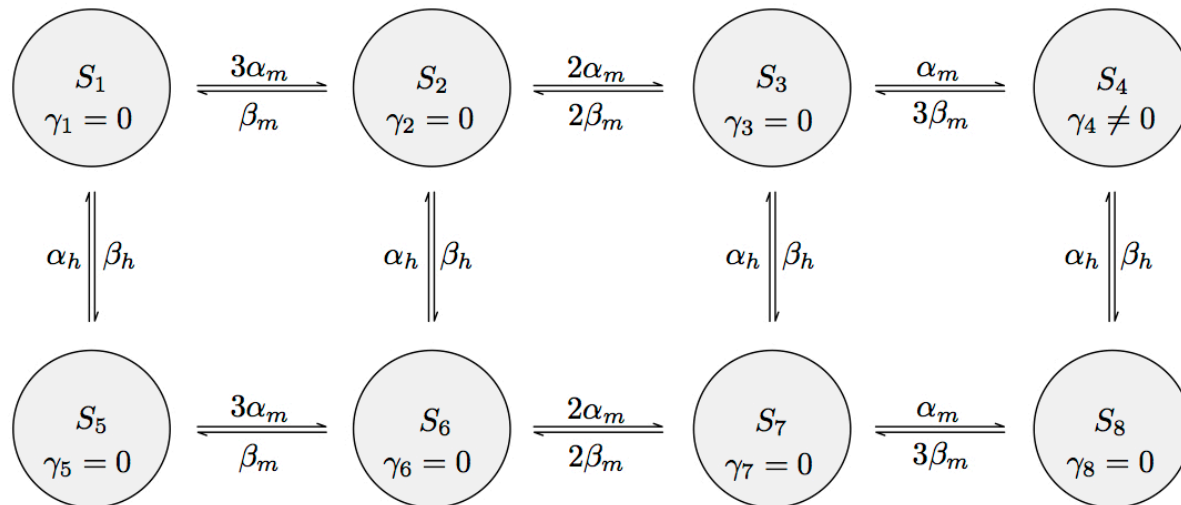


Figure 6.56

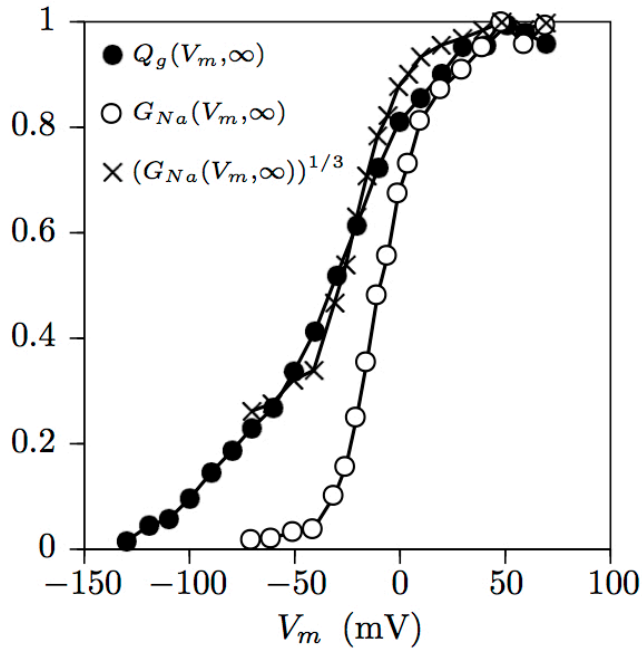


Figure 6.57

Conductance voltage-dependence consistent w/ HH if there are three independent activation gates (i.e., m^3)

HH predicts values for the various time constants...

... that are inconsistent with data ("tail currents")

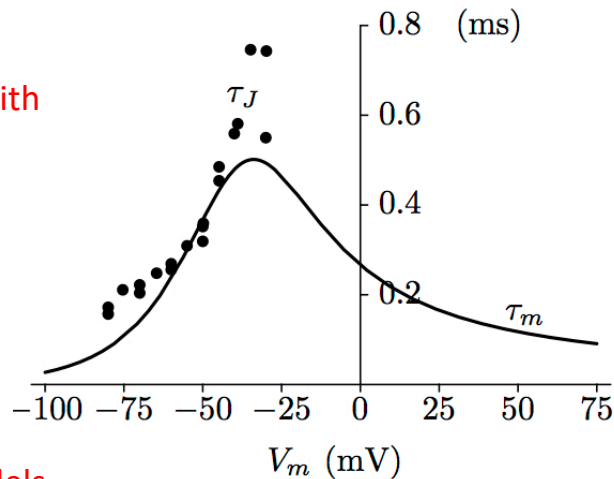


Figure 6.59

→ Four independent two-state models still too simple. Multi-state channels?

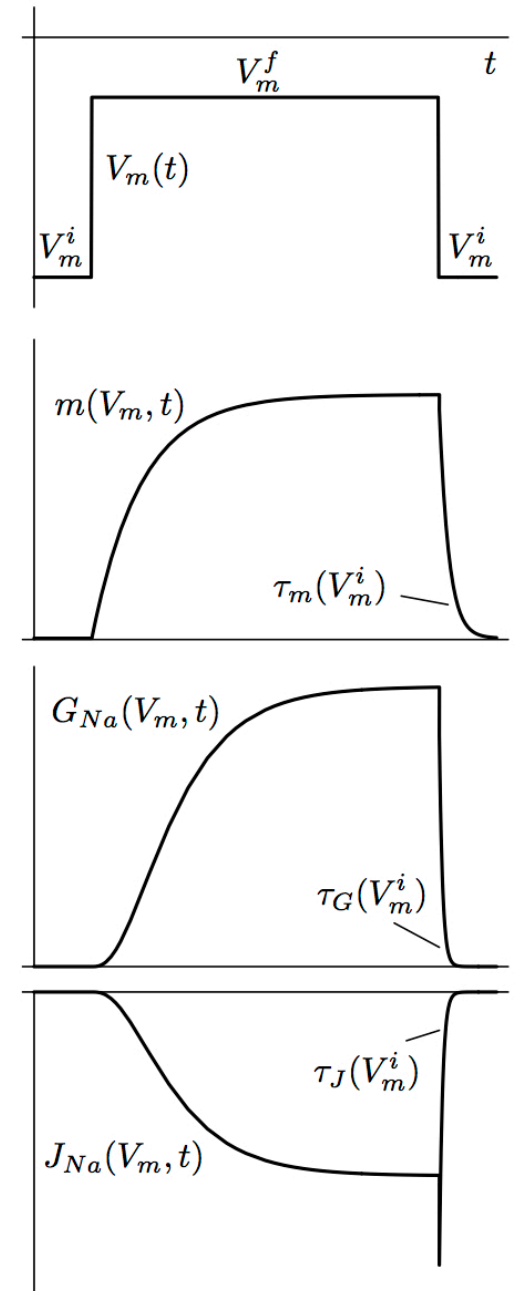


Figure 6.58

Multistate Channel Models

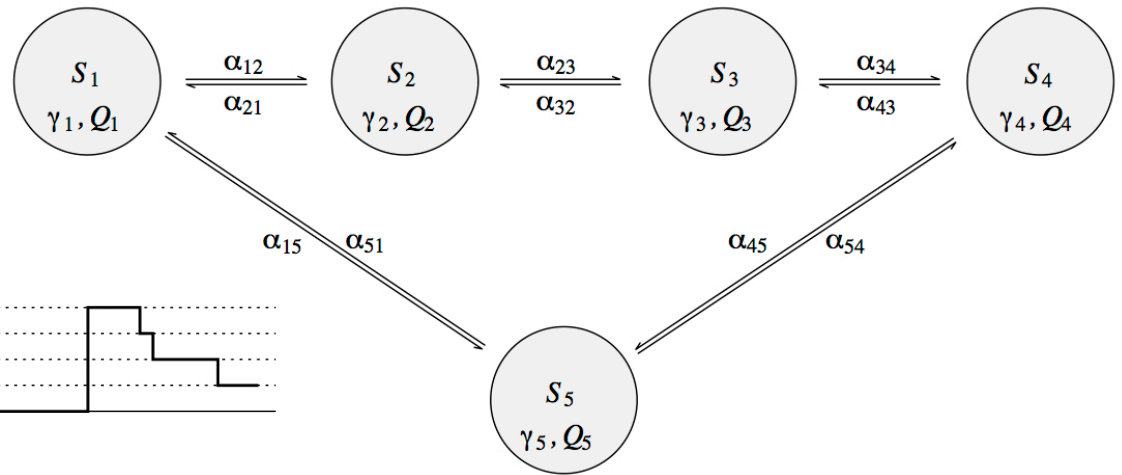


Figure 6.60

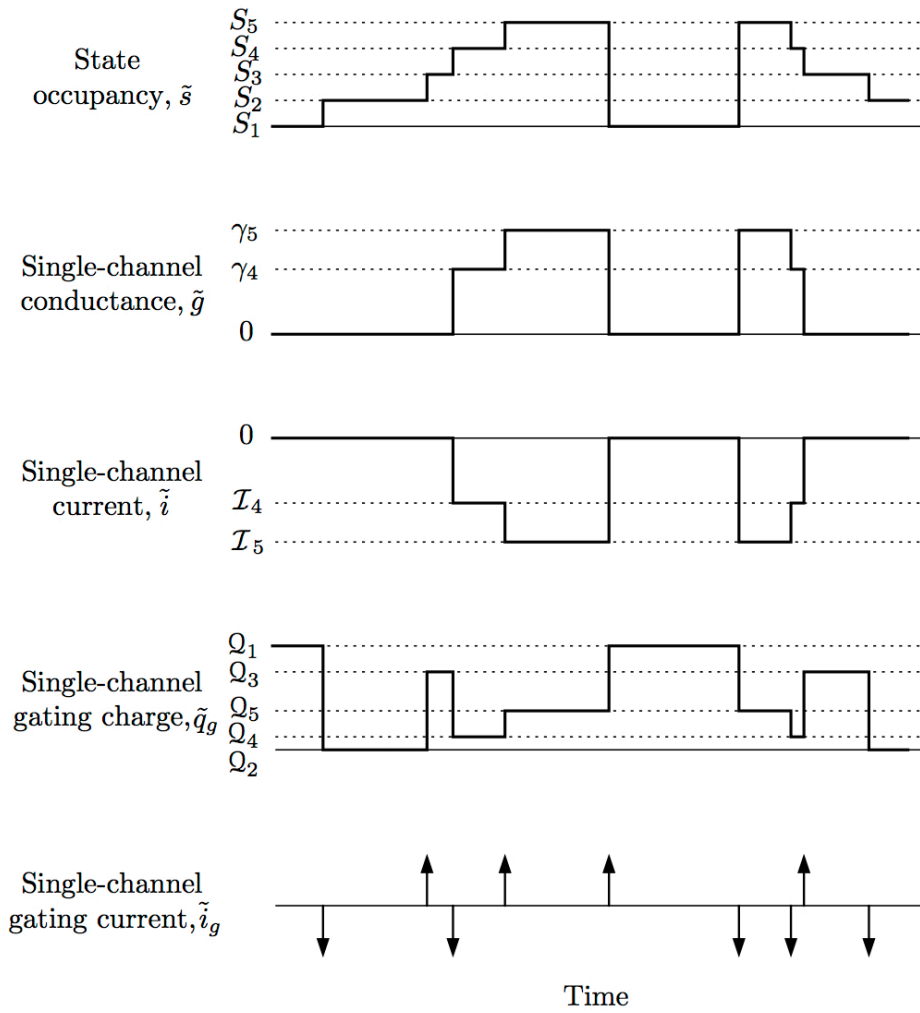


Figure 6.61

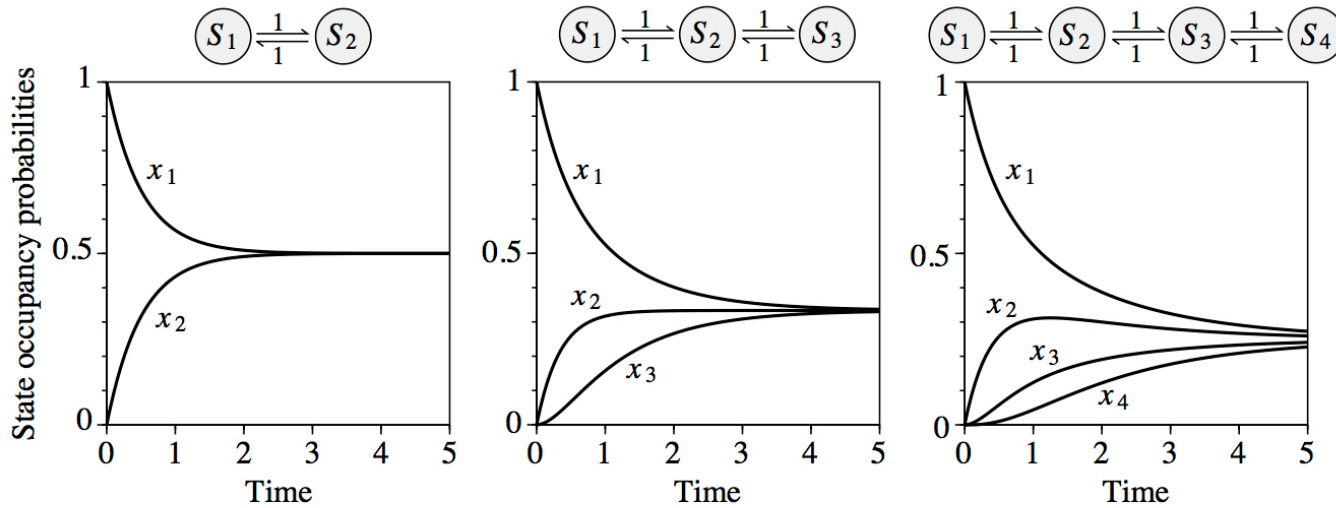
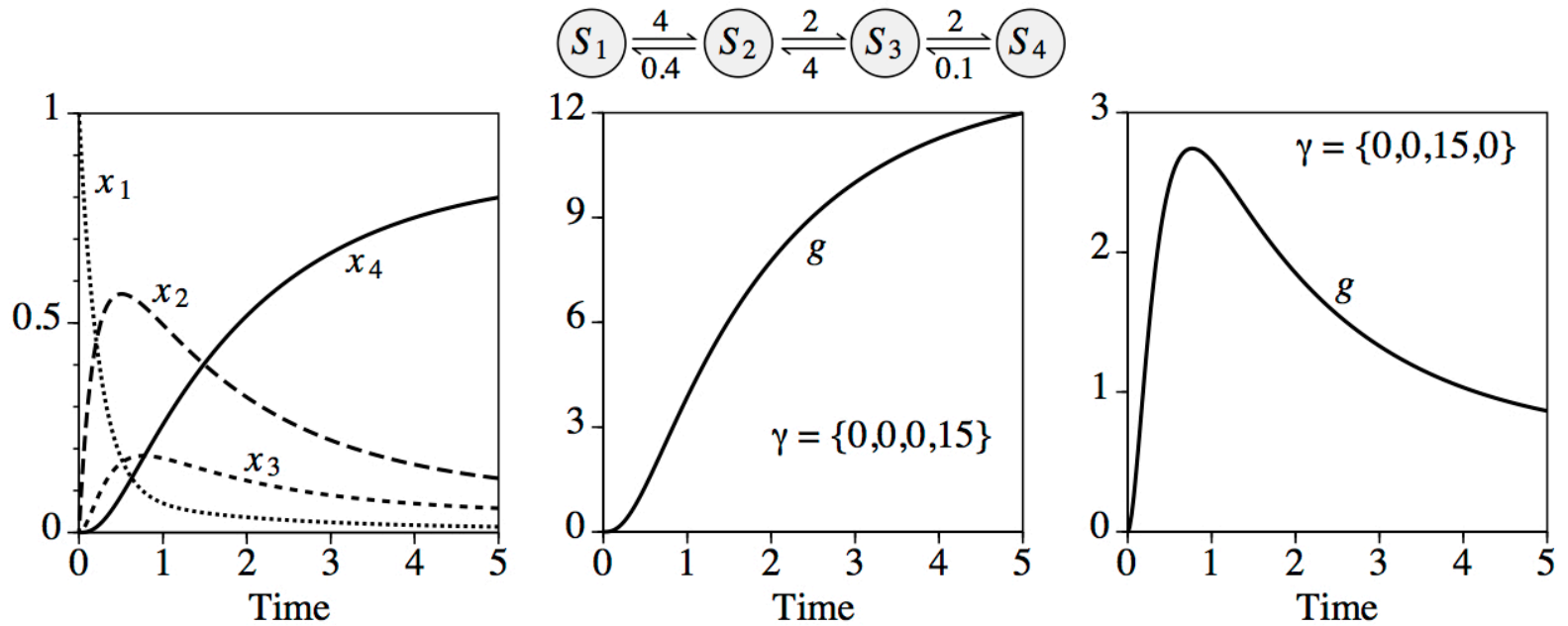


Figure 6.62

→ s-shape stems from “lag incurred by the state occupancy having to traverse earlier stages”



Molecular Underpinnings

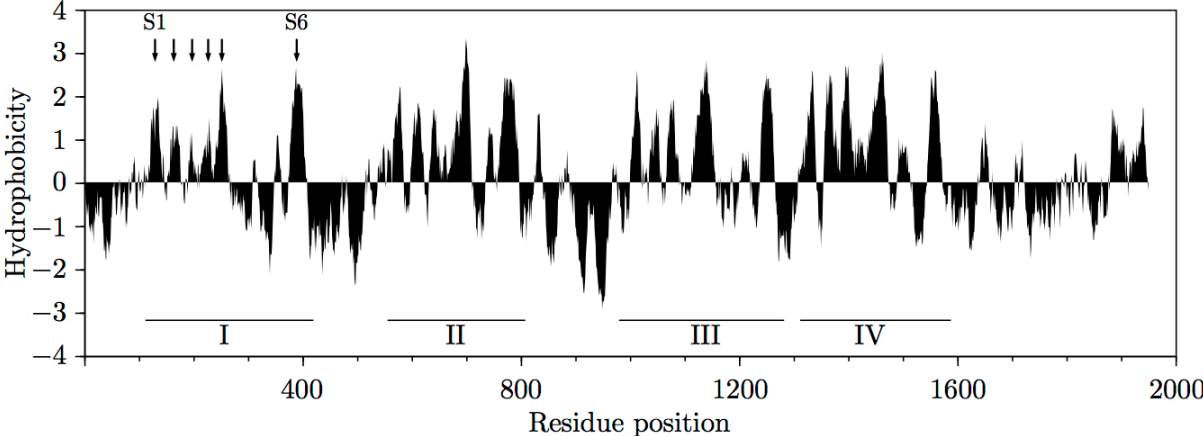


Figure 6.68

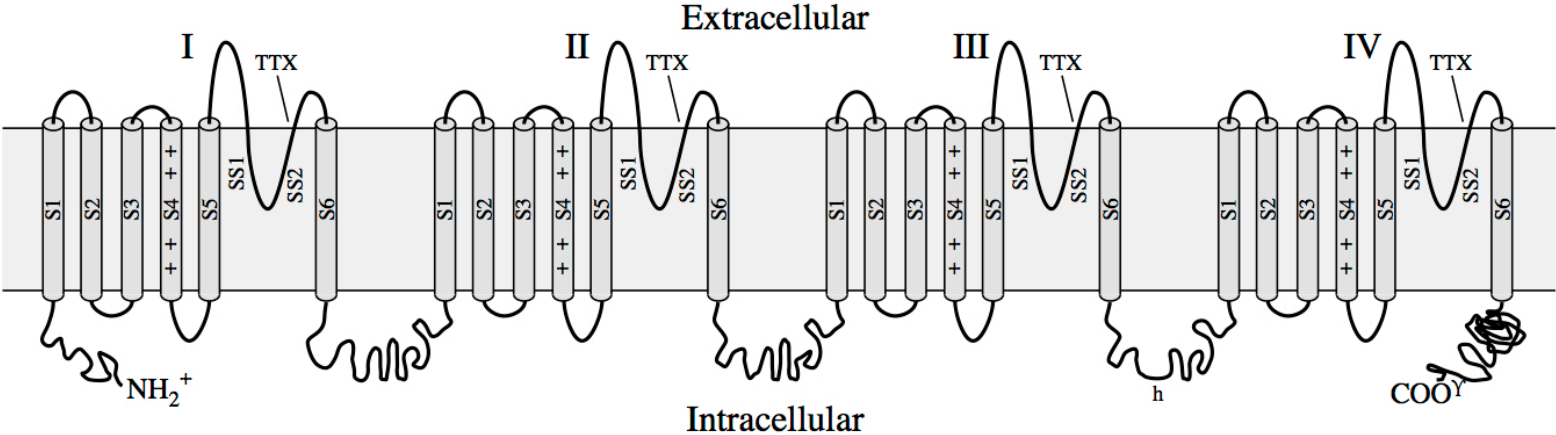


Figure 6.69

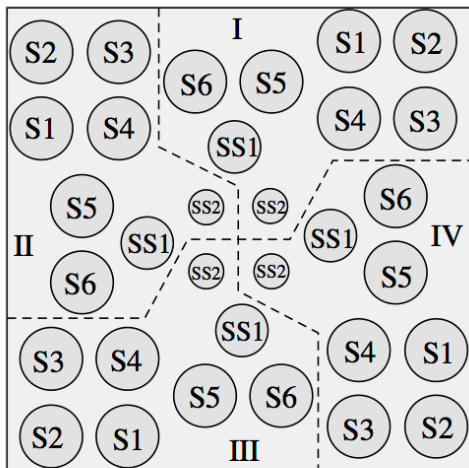
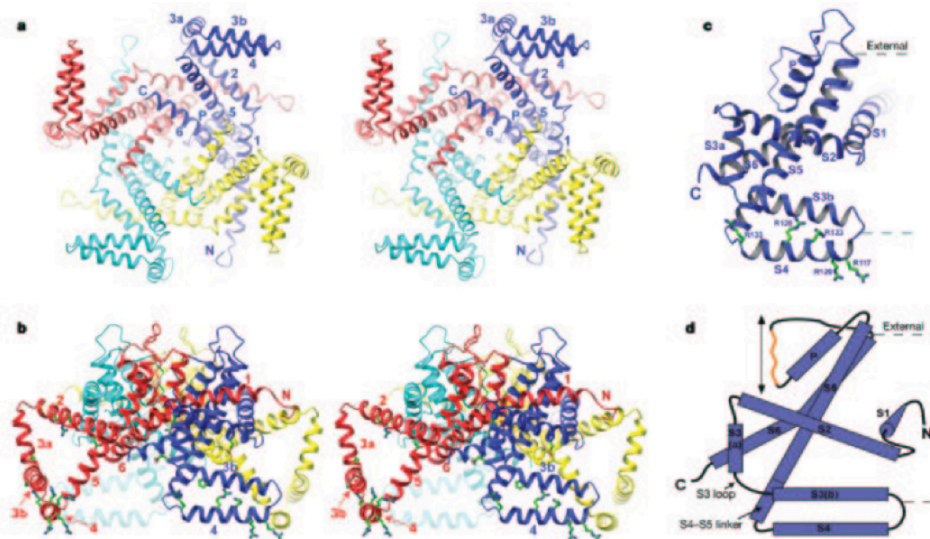
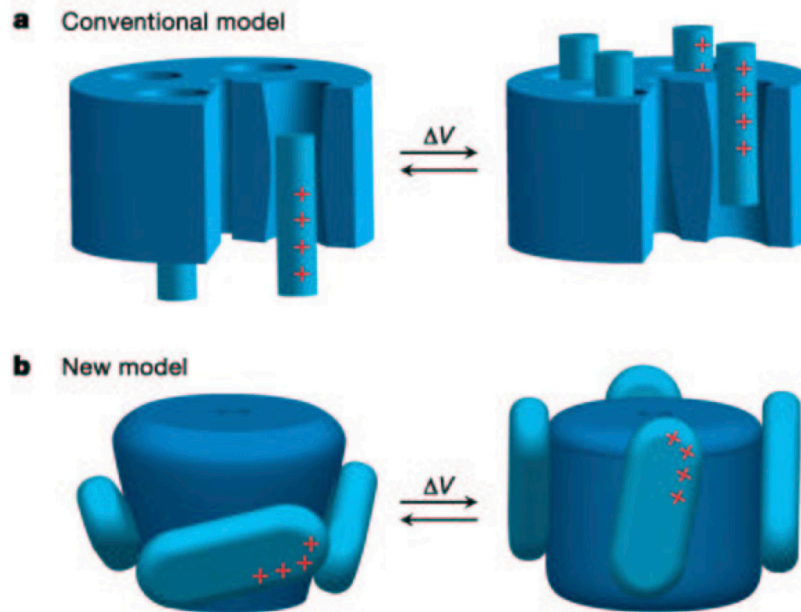


Figure 6.70



Y. Jiang, A. Lee, J. Chen, V. Ruta, M. Cadene, B. Chalt, and R. MacKinnon (2003),
Nature 423:33-41.



Y. Jiang, A. Lee, J. Chen, V. Ruta, M. Cadene, B. Chalt, and R. MacKinnon (2003),
Nature 423:33-41.

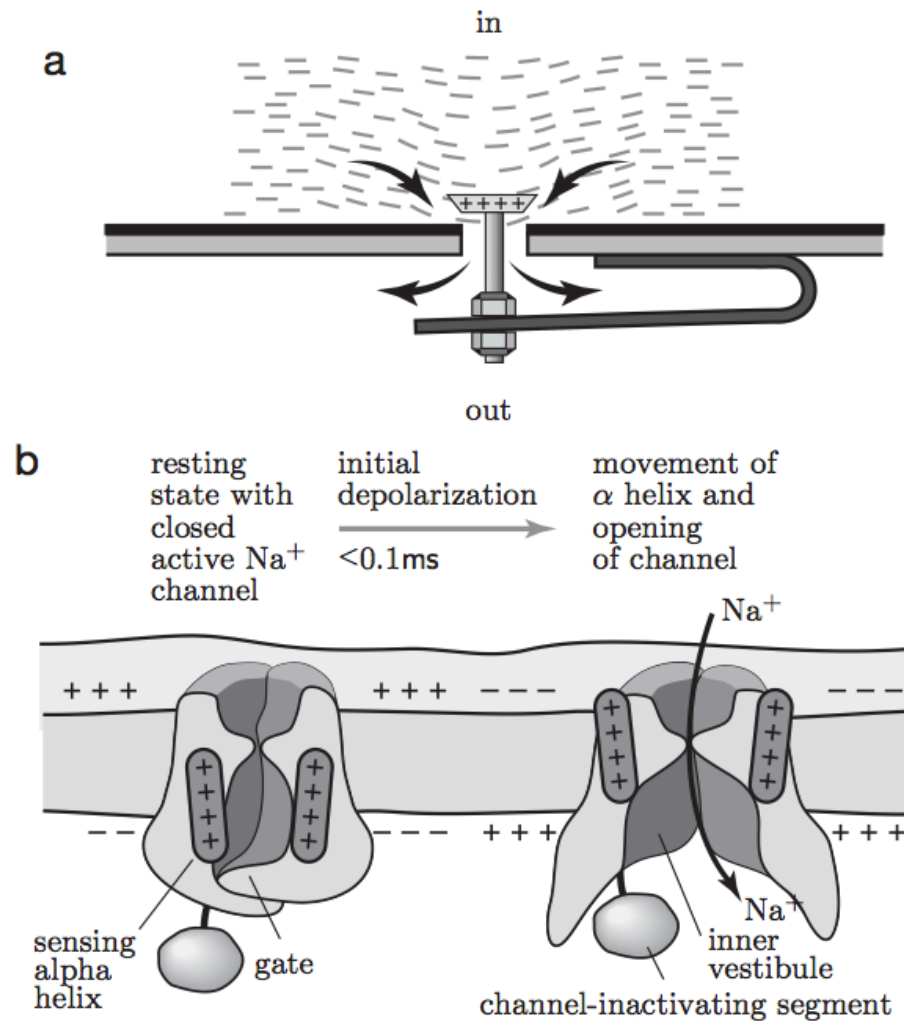


Figure 12.16: (Schematic; sketch.) (a) Conceptual model of a voltage-gated ion channel. A spring normally holds a valve closed. An electric field pointing upward lifts the positively charged valve, letting water flow downward. (b) Sketch of the sodium channel. *Left:* In the resting state, positive charges in the channel protein's four "sensing" alpha helices are pulled downward, toward the negative cell interior. The sensing helices in turn pull the channel into its closed conformation. *Right:* Upon depolarization, the sensing helices are pulled upward. The channel now relaxes toward a new equilibrium, in which it spends most of its time in the open state. The lower blob depicts schematically the channel-inactivating segment. This attached object can move into the channel, blocking ion passage even though the channel itself is in its open conformation. [After Armstrong & Hille, 1998.]